

## 27. LATE CRETACEOUS VOLCANICLASTIC ROCKS FROM THE WALVIS RIDGE, SOUTHEAST ATLANTIC, LEG 74<sup>1</sup>

M. Simon and H.-U. Schmincke, Institut für Mineralogie, Ruhr-Universität, D-4630 Bochum, Federal Republic of Germany

### ABSTRACT

Volcaniclastic rocks of Late Cretaceous age occur in four out of five sites (525, 527, 528, 529) drilled on the crest and the northwest flank of the Walvis Ridge during Leg 74. They are mostly interlayered with and overlie basement in the lowermost 10–100 m of the sedimentary section. Rocks from Holes 525A and 528 were studied megascopically and microscopically, by XRD, and XRF chemical analyses of whole-rock major and trace elements were undertaken. The dominant rock of Hole 528 volcaniclastics is a fine-grained (silt to fine sand), mostly matrix-bearing (partly matrix-rich) vitric "tuff," occurring as 5–110 cm thick, partly graded layers, some of which are distinctly bedded. Volcaniclastics of Hole 525A are generally richer in sanidine crystals. Most rocks contain some nonvolcanic clasts, chiefly foraminifers and lesser amounts of shallow-water fossil debris. Scoria shards, clasts of tachylite, and fine-grained basalts as well as chemical analyses suggest a basaltic to intermediate composition for most rocks of Hole 528, whereas volcaniclastics of Hole 525A are more silicic. The occurrence of tachylite and epiclastic, coarse-grained, basaltic clasts throughout the volcaniclastic sequence at Site 528 indicates shallow-water eruptions and perhaps even ocean island volcanism. The minor occurrence in Hole 528 of trachytic? pumice shards with phenocrysts of K-feldspar and the abundance of such shards in rocks from Hole 525A indicate Plinian eruptions characteristic of more mature stages of ocean island evolution. The sedimentary structures of volcaniclastic layers and their occurrence within deep sea calcareous oozes indicate a mass flow origin.

Diagenetic alteration of the volcaniclastic rocks is pronounced, and four major stages of glass shard alteration are distinguished. Despite the effects of alteration and small-scale redistribution of elements and the admixture of nonvolcanic components, there were no drastic changes in the chemical composition of the rocks, except for pronounced increases in K and Rb and decreases in Ca and Fe. The basaltic volcaniclastic rocks very much resemble basement basalts in that they are moderately evolved tholeiites derived from an LIL-enriched mantle source with Zr/Nb ratios (Hole 528) of 5 to 6. This, in conjunction with the interbedding of volcaniclastic rocks and basement lavas, indicates contemporaneous seamount or island and basement volcanic activity involving magmas derived from similar sources.

### INTRODUCTION

At the five sites (525–529) drilled during Leg 74 in the Eastern South Atlantic, situated at present water depths between 1054 m and 4428 m, sediments range in age from Pleistocene to Late Cretaceous (Maestrichtian and, in Hole 525A, Campanian) (Figs. 1–3). Basement was cored at three sites. Downward in most holes the sediments change in composition from nannofossil and foraminiferal-nannofossil ooze to chalk, interlayered near the base at three sites (525, 528, 529) with volcaniclastic sediments of Late Cretaceous to early Paleogene age. Volcaniclastic sediments and nannofossil chalk and limestone also occur sandwiched between basement basalt sheets and pillow flows. The basalts are tholeiitic (MgO 6.5 to 4.5%) and enriched in incompatible elements compared to "normal" MORB (Richardson et al., this volume).

In this chapter we have studied volcaniclastic rocks in order to contribute to understanding of the origin and evolution of the Walvis Ridge. For example, were the volcaniclastic sediments derived from seamounts or true subaerial islands? Did these islands or seamounts resemble the basement chemically, and is this association of rift basement and large central volcanic edifice similar

to such present-day examples as Iceland or the Azores? Can the volcaniclastic sediments be related to particular stages in the evolution of a seamount or island, and is this relationship reflected in the vesicularity and abrasion history of the volcanic clasts? Related questions concern the distance to the volcanic source area, the mode of transport, and the duration of the volcanic and erosional processes at the source area as they are reflected in the stratigraphic and geographic distribution of the volcaniclastic sediments. Finally, alteration textures and the minerals and bulk chemistry of the volcaniclastic components may give important clues to the diagenetic history of the sediments during the last 70 m.y.

### METHODS

From Holes 525A and 528, 41 samples were studied (see Figs. 3–4). Thin sections were prepared from resin-hardened samples. X-ray diffraction analyses were carried out for whole rock samples and for carbonate and organic-free residues, using a Phillips diffractometer with  $\text{CuK}\alpha$  radiation. A few polished thin sections were used for cathodoluminescence studies using techniques described in Zinkernagel (1978). Thirteen samples were chemically analyzed for both major and trace elements by X-ray fluorescence methods on glass fusion beads using a fully automatic Phillips PW 1400. The fusion beads consist of rock powders (dried at 110°C overnight) and flux (lithium metaborate and dilithium tetraborate, Merck A 12) in the ratio of one part rock to four parts flux, melted at 1000°C for 20 min. and poured into a 34-diameter pellet mold. The sample was digested in hydrofluoric acid-silver perchlorate. FeO was determined by semiautomatic potentiometric titration with a standard potassium bromide solution;  $\text{CO}_2$  by closed-system coulometric titration of a barium perchlorate solu-

<sup>1</sup> Moore, T. C., Jr., Rabinowitz, P. D., et al., *Init. Repts. DSDP, 74*: Washington (U.S. Govt. Printing Office).

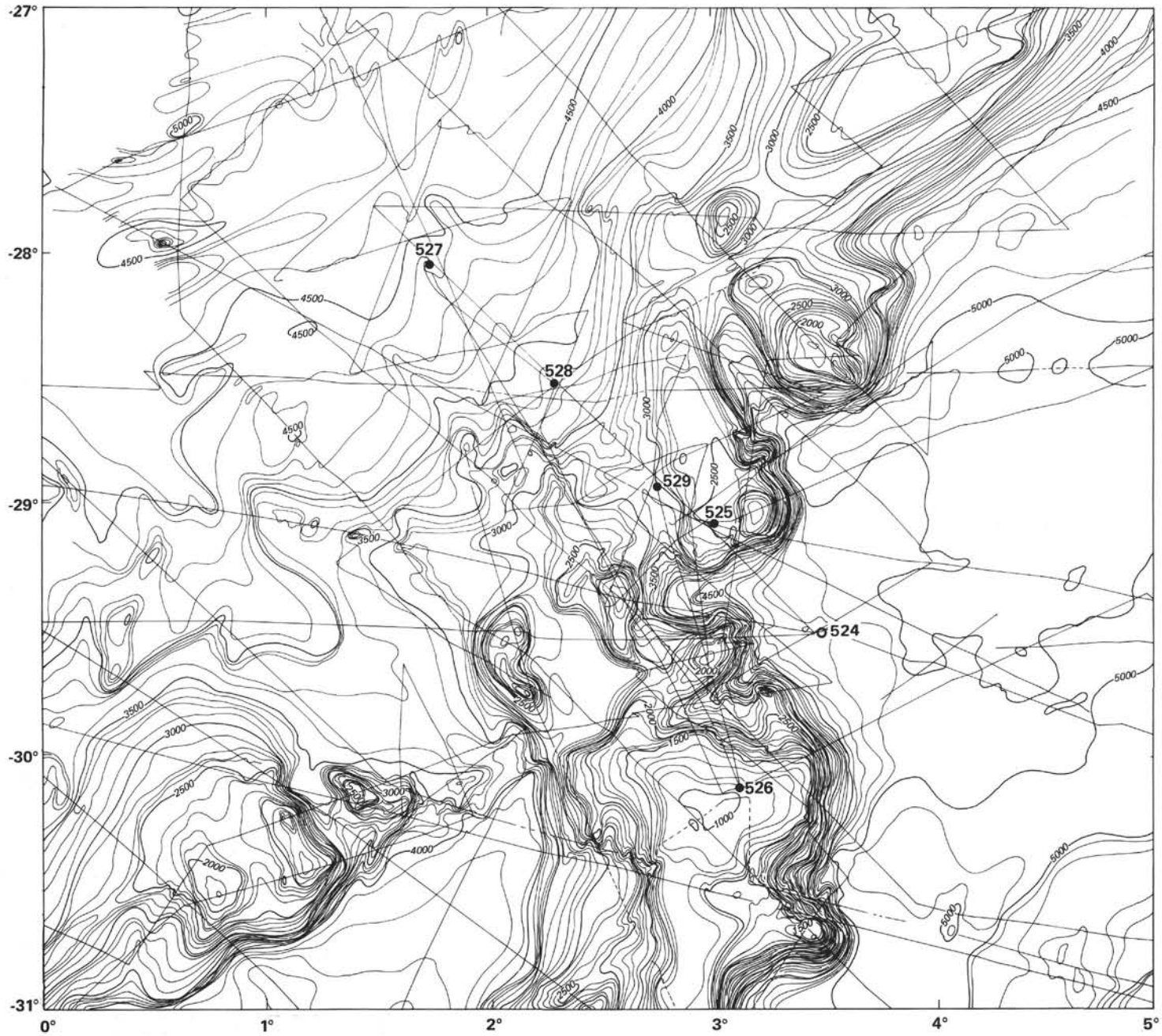


Figure 1. Bathymetric map of Leg 74 drilling area. Open circle shows Leg 73, Site 524.

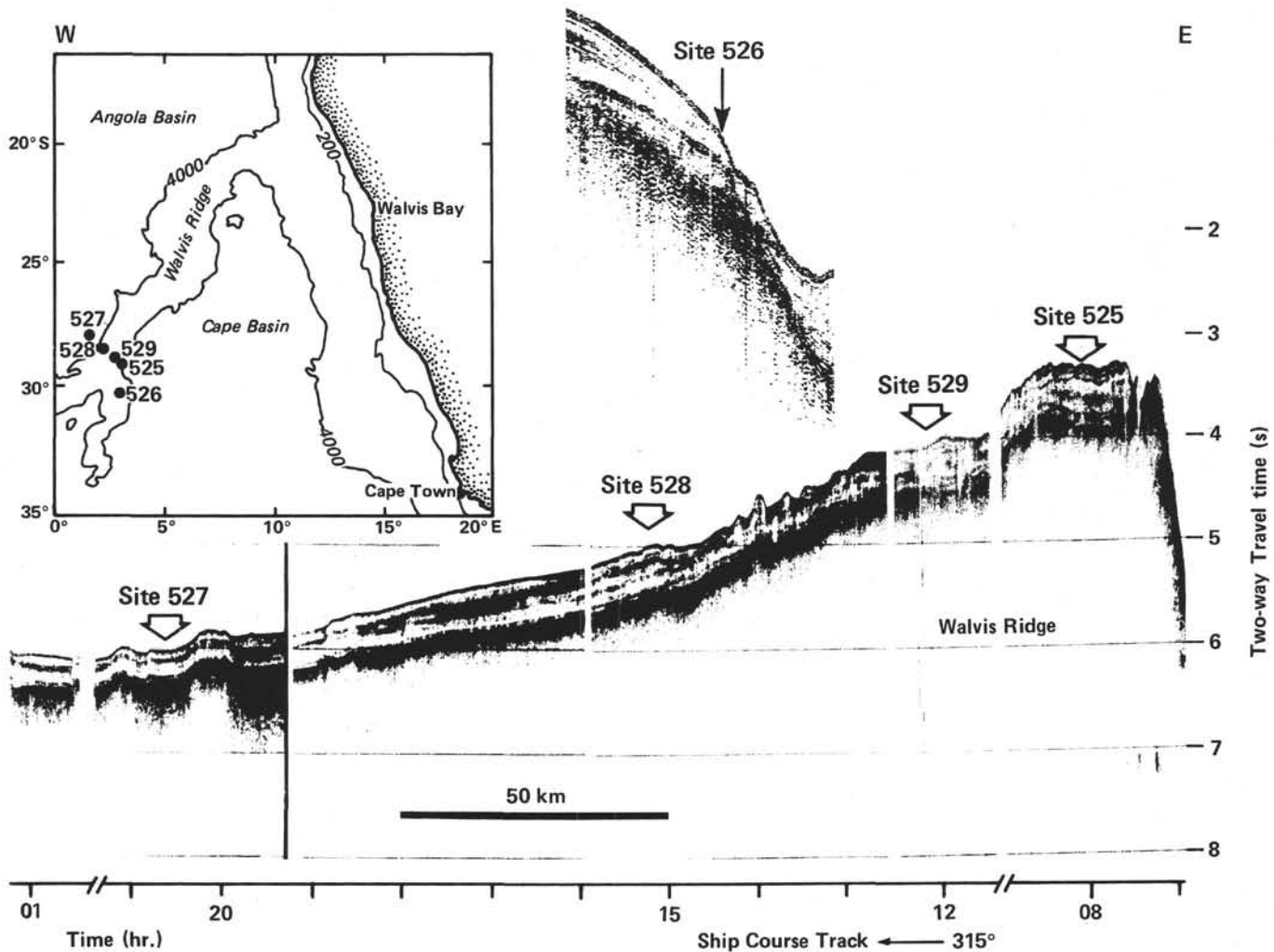


Figure 2. Seismic profile of the Walvis Ridge transect, showing Leg 74 site locations.

tion into which were passed the gases produced by passing oxygen over the sample roasted in a tube furnace; and  $H_2O^+$  by closed-system coulometric titration of a nonaqueous Karl-Fischer reagent into which was passed the inert carrier gas (nitrogen) containing water which was stripped from the sample by heating it in a Pt-crucible to  $1300^\circ C$  with an induction furnace.

### MACROSCOPIC DESCRIPTION OF VOLCANICLASTIC ROCKS AND THEIR DISTRIBUTION THROUGHOUT HOLES 525A AND 528

#### Macroscopic Description

Most volcanoclastic rocks are only slightly indurated, although a few are well cemented. Rocks are predominantly greenish gray to olive black. Yellowish or light gray zones occur at the contacts to under- and overlying sediment, probably because of incorporated lutitic matrix. Lutite at the base was obviously incorporated during transport of the volcanoclastic material by mass flows, whereas lutite in the top zone of a volcanoclastic layer may be due to burrowing. Coarse-grained samples have an olive greenish matrix, contrasting with the white feldspar clasts and light-colored rock fragments. In Sample 528-37-1, 135–138 cm (Plate 1, Fig. 2) these clasts are slightly enriched at the base of the volcanoclas-

tic layer. Light-colored clasts consist of plagioclase and K-feldspar, and massive lithic clasts are possibly of trachytic composition. Dispersed throughout the coarse layer of Sample 528-37-2, 37–40 cm (Plate 1, Fig. 1) are light-colored clasts up to 7 mm in diameter. Feldspar clasts in this sample are mostly strongly altered and hollow-centered. Dark lapilli-sized particles are either tachylite or smectite-replaced glass shards, both showing considerable vesicularity. Some fine-grained, silty rocks are well bedded and show white areas, either parallel to bedding or patchy, generally representing strongly zeolitized or, rarely, carbonatized areas (Plate 1, Figs. 3 and 4). White zeolitized glass shards are macroscopically recognizable in a few rocks.

#### Site 525: Distribution of Volcanoclastic Rocks

At this site volcanoclastic rocks occur between 460 and 650 m sub-bottom, interbedded in the lower part with basalt lava flows and nanofossil chalk (Fig. 3). A thick turbidite sequence ( $>4$  m) with minor amounts of volcanoclastic components occurs 5.5 m above basement in Core 525A-52. Overlying sediments contain only small, gray green volcanoclastic layers, and volcanoclastic material occurs dispersed within the nanofossil ooze

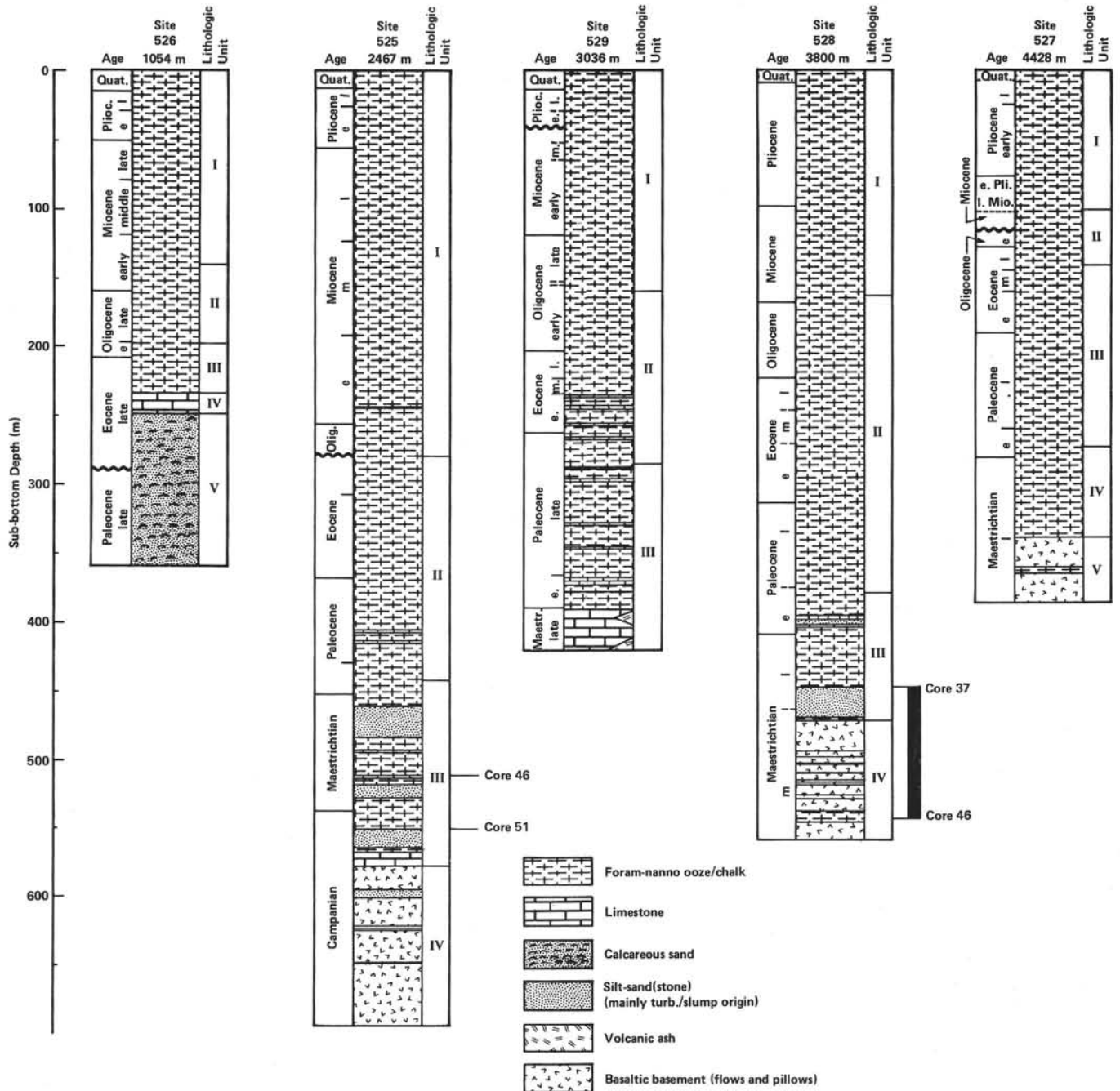


Figure 3. Stratigraphic and lithologic columns of Leg 74 sites.

and chalk. The sandy to silty volcanoclastic rocks which occur in the lowermost 105 m of the sedimentary section above basement were interpreted by the shipboard party as small-scale slumping deposits (see site report, this volume). Our samples in Hole 525A are from Cores 51 and 46, at 16.5 and 60–63 m above basement and at 557 and 508–511 m sub-bottom depth, respectively. They are highly bioturbated gray greenish nannofossil chalks with lenses of olive-colored sands and silts of volcanic material (Samples 525A-46-1, 48–55 cm, 525A-46-4, 42–45 cm, and 525A-46-4, 45–53 cm). Sample 525A-46-4, 45–53 cm contains feldspar clasts up to 5 mm in diame-

ter in a coarse sandy layer, together with pale olive green clasts of clay minerals (Plate 1, Fig. 5). The lowermost sample of this hole shows silt-sized volcanic and carbonate particles (e.g., shell fragments of *Inoceramus*) in a distinct layer, about 5 cm wide, sandwiched between silty nannofossil–foraminifer ooze.

**Site 528: Distribution of Volcanoclastic Rocks**

Volcanoclastic rocks drilled at Site 528 occur in three main units, interbedded with both basement basalt and foraminifer–nannofossil ooze (Fig. 4). They are dominantly sand-sized, in part silt-sized, with a few layers of

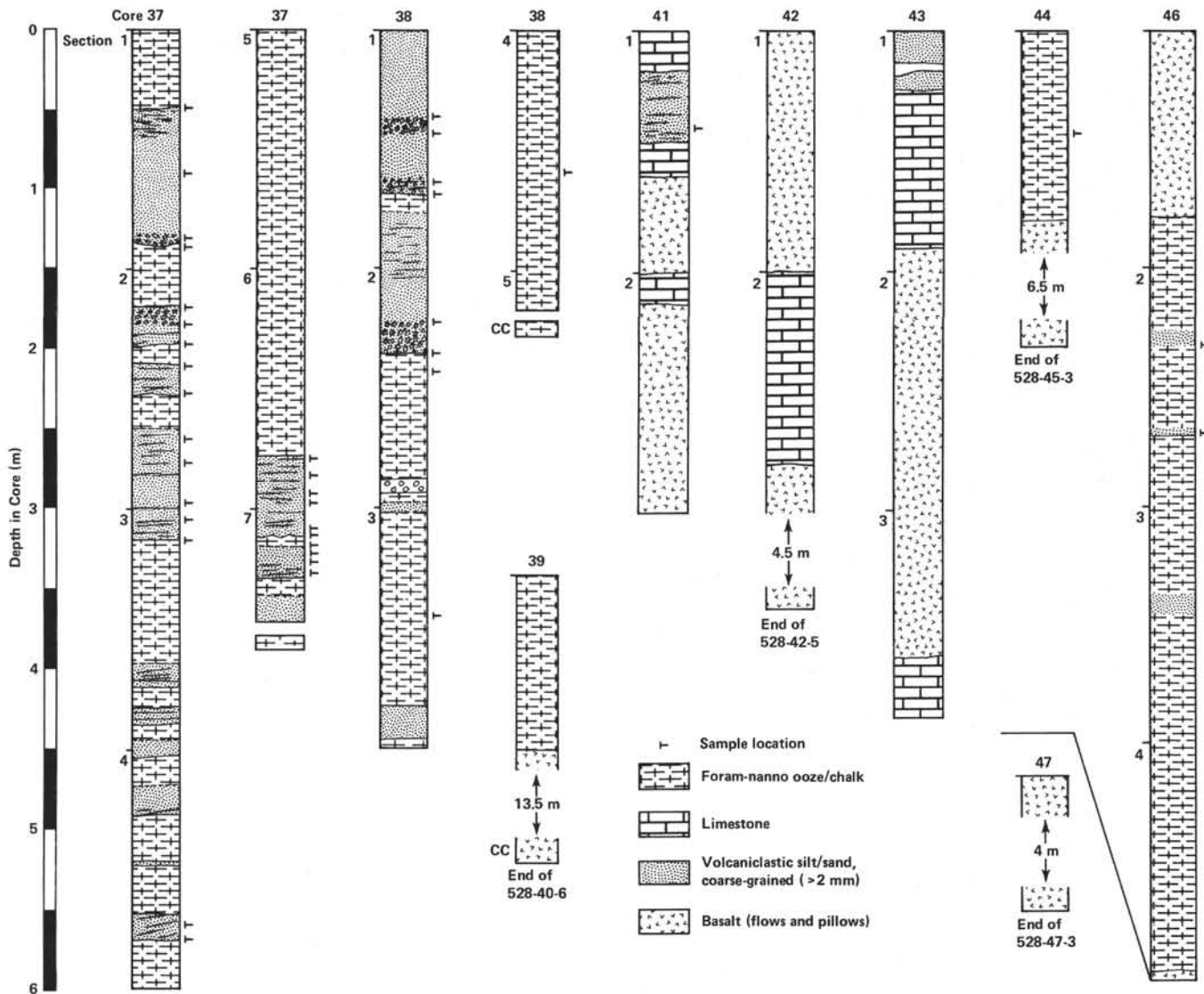


Figure 4. Lithology and sample location of Cores 37-46 of Hole 528, showing volcaniclastic rocks interlayered with basalt and nannofossil chalk.

coarser grain-sized materials. The oldest volcaniclastic rocks cored at this site occur in Core 528-46, where they are intercalated within about 5 m of nannofossil ooze which itself is sandwiched between basaltic flows. Two further volcaniclastic layers (0.4 and 0.5 m thick), together with under- and overlying limestones, are interbedded with basalt flows at 35 m and 18 m below the top of the basement (Cores 528-43 and 528-41). Sedimentary structures of these greenish gray sandstones and siltstones are typical of turbidite deposits. The lack of the coarse-grained basal layer (layer a of the Bouma cycle) suggests a distal facies of a turbidite (see site report, this volume).

The second unit of volcaniclastic rocks begins 3 m above the top of the basalt flows. Its lower part consists of 3 thin layers (< 20 cm thick) interbedded with 2 m of nannofossil chalk. The main volcaniclastic part of this unit occurs at the top of Core 528-38 and in the lowermost 1 m of Core 528-37 (Fig. 4). It is made of three layers, each about 1 m thick, which are separated by minor pelagic sediment. These layers are normally to inversely

graded and are greenish black in color. They are also interpreted as mass flow deposits. This volcaniclastic sequence is separated from the topmost unit by 3 m of nannofossil chalk (mostly in Sections 528-37-5 and 528-37-6). The third unit of volcaniclastic rocks occurs in Sections 528-37-1 to 528-37-4). Volcaniclastic layers range in thickness from 5 to 80 cm and were also interpreted as turbidites by the shipboard party (see site report, this volume).

Volcaniclastic sediments of Unit 1 make up 12% of the lowermost 55 m of Hole 528, compared to 23% of "normal" sediment (nannofossil and/or foraminiferal ooze? chalk) and 65% of basalt. Above basement, volcaniclastic sediments of Units 2 and 3 occur in the interval from 454.5 to 478.5 m sub-bottom. The sediments of this interval are dominated by nannofossil chalk with 37% volcaniclastic rocks. Within this interval above basement, two maxima of volcaniclastic sedimentation are present (Units 2 and 3; Fig. 5). At a sediment accumulation rate of  $2 \text{ cm}/10^3 \text{ y}$ . (calculated from the ship-

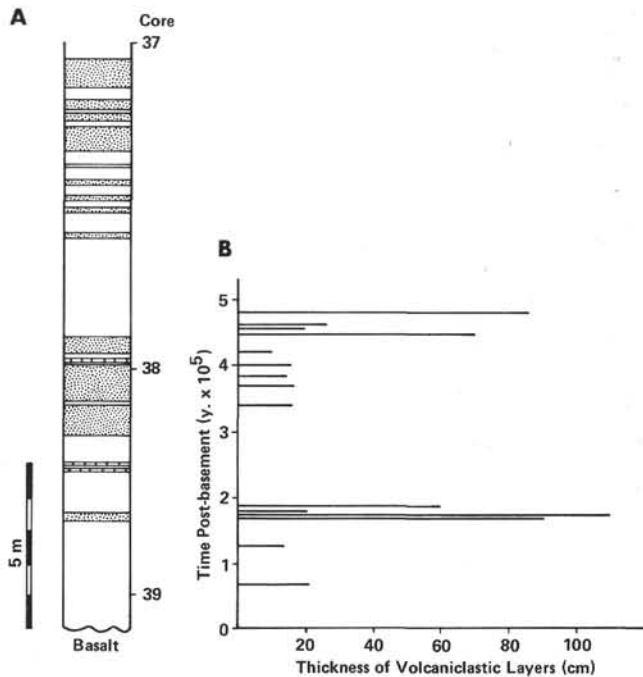


Figure 5. Volcaniclastic rocks of the lower part of Hole 528, interlayered with nannofossil chalk/ooze above basement. A. Sedimentary column showing thickness and abundance of volcaniclastic layers (stippled). B. Thickness of volcaniclastic layers versus time. Two distinct maxima of volcaniclastic sedimentation, each finishing with thick layers, are recognizable.

board estimate of the carbonate accumulation rate and from the compaction of the nannofossil sediments) this 24-m thick interval would comprise nearly 0.5 m.y. Above this interval, the volcaniclastic sedimentation has practically terminated. In Core 528-36, two further small layers of volcaniclastics occur, each less than 20 cm thick. No more volcaniclastic layers are reported by the shipboard party in the upper part of the section.

## PETROGRAPHY OF VOLCANICLASTIC ROCKS

### Primary Components and Their Alteration

Volcaniclastic rocks are composed primarily of (a) vitric, lithic, and crystal clasts of volcanogenic origin, (b) nonvolcanic clasts, mostly biogenic and predominantly foraminiferal and (c) groundmass of clay and carbonate ooze. Estimated proportions of these components are shown in a ternary diagram (Fig. 6A), which shows most rocks to be groundmass-bearing volcaniclastic rocks with only minor amounts of nonvolcanic clasts like biogenic debris.

A few samples with more than 20% biogenic components are mostly from the uppermost parts of volcaniclastic layers. Fossils are predominantly foraminifers, and, more rarely, fragments of molluscan shells, bryozoans, coralline algae, and echinoderms. Foraminifers are occasionally enriched in layers up to 5 mm thick, where they are the only biogenic clast (e.g., Sample 528-37-2, 97–101 cm). Some groundmass-rich layers are either from the base of a volcaniclastic rock, where ooze from the underlying sediment may have been inworked

during transport, or from the tops of layers, which are often strongly disturbed by burrows.

## Volcanic Clasts

### Vitric Clasts

Former glass shards, now strongly altered, are the dominant volcanic component in most volcaniclastic rocks (Fig. 6B). They comprise a wide range of size, shape, and vesicularity and are divided into three main groups: pumice, scoria, and spalling shards. Exact discriminations between these three types should be based upon shard outline, vesicularity, shape and diameter of vesicles, thickness of walls between vesicles, and other

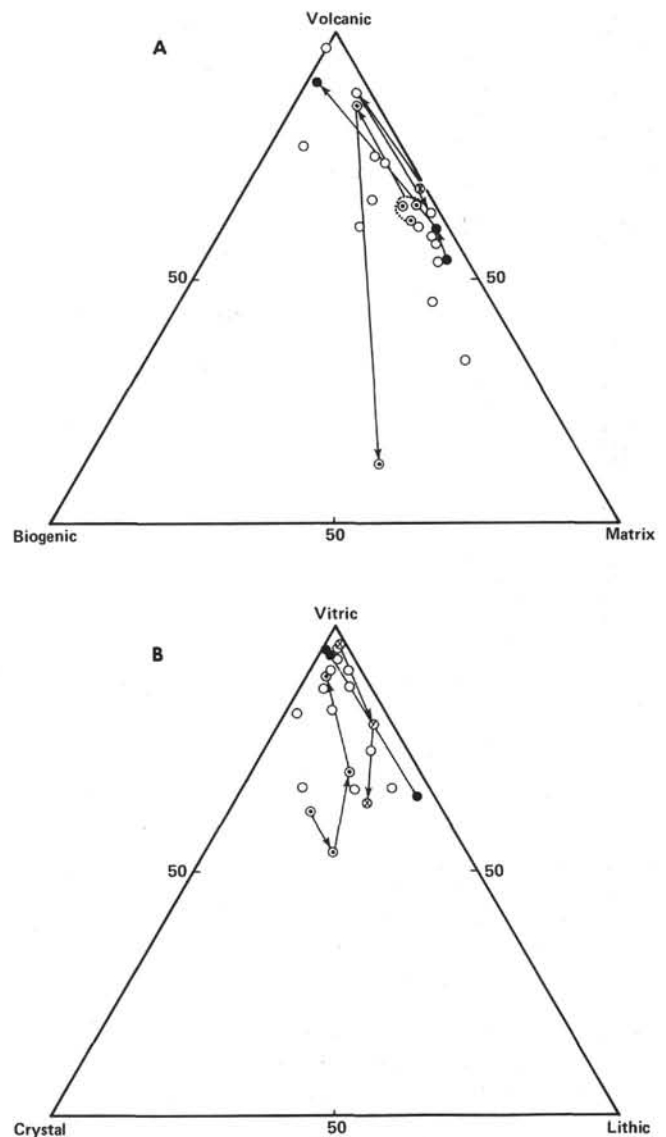


Figure 6. A. Ternary plot of primary components of Hole 528 volcaniclastic rocks. Tie-lines connect samples of one layer (arrows point towards overlying sample) ⊗ 528-37-2, 50–52 cm to 528-37-2, 37–40 cm, B ⊙ 528-37-3, 18–20 cm to 528-37-2, 97–101 cm ● 528-37-1, 135–138 cm to 528-37-1, 49–51 cm. B. Ternary plot of volcanic particles of volcaniclastic rocks from Hole 528. Tie-lines and symbols as for A.



filling of the void by secondary minerals. These two alteration types may occur one after the other within one shard. Alteration of basaltic to intermediate scoria shards seems dominated by *in situ* transformation.

Hydrated glass as well as highly altered and partly dissolved "residual" shards show light to dark brown rims of iron and/or manganese (and titanium?) oxides? (hydroxides), partly admixed with fine-grained, granular, light brown crystals (smectite?),  $< 1 \mu\text{m}$   $\phi$ . Rims are  $< 1\text{--}2 \mu\text{m}$ , rarely up to  $5 \mu\text{m}$  thick, and affect all types of shards. The rims may represent either a coating or a replacement of the glass; their commonly sharp boundary toward the interior of the shard and their less distinct outer limit suggest a coating. These rims are distinguished from the dark brown groundmass rims around particles (see later) by their lighter color and the absence of spheroidal textures. Toward the interior of the shard, the "coatings" are succeeded by light brown rims of equigranular smectite (crystals  $< 1 \mu\text{m}$   $\phi$ ) which are easily recognized by their distinct birefringence, whereas the "coatings" are nearly isotropic. The smectite rims range in thickness from  $1 \mu\text{m}$  to, most commonly,  $3\text{--}10 \mu\text{m}$ , and rarely fill an entire shard. This microgranular smectite generally surrounds all surfaces of shards, including outer surface and internal bubble walls, and may be succeeded by fibrous or bladelike smectite.

In a few samples, well-developed smectite crystals border the inner and outer shard wall and both sides of vesicle walls in the form of  $5\text{--}10 \mu\text{m}$  (up to  $15 \mu\text{m}$ ) thick rims. Spherical bunches of light yellow to light green fibrous smectite crystals surround former microvesicles or microphenocrysts in the glass. The smectite crystals are very thin (generally  $< 1 \mu\text{m}$ ) and appear in thin section as acute, long needles  $5\text{--}10 \mu\text{m}$  long, exhibiting extremely sharp points toward the interior of the shard or pore space. Most shards with this type of alteration are either center-hollowed or totally smectitized. Fibrous smectite occurs within all types of shards but is mostly found in well-sorted "tuff" layers of spalling shards, as, for example, Sample 528-37-7, 42–46 cm, where a tuff layer marks the base of a volcanoclastic deposit (Plate 2, Figs. 1 and 2).

In some shards, pale yellowish to colorless fibrous crystals coating the inner shard walls appear as  $10\text{--}15 \mu\text{m}$  thick palisades, the crystals being much more closely packed than the fibrous smectite (Plate 5, Fig. 1). The mineral is only very weakly birefringent; its refractive index lies much above that of phillipsite and it is presumably a zeolite, perhaps thomsonite?. Because it occurs only in very small amounts and sizes, it cannot be identified in whole rock XRD diagrams or by single-crystal XRD. The thomsonite? palisades are generally overgrown by long, thin fibers of phillipsite, also partly palisadelike. Phillipsite largely or entirely replaces the glass, having grown from all sides of its base toward the interior. Shards with fibrous smectite palisades generally lack fibrous phillipsite. Shards without the fibrous smectite and thomsonite? mostly have a rim of phillipsite, grown directly upon the light brown rim of granular smectite. This phillipsite is not fibrous but is still needle-like (Plate 5, Fig. 2). Some phillipsite builds up semi-

spherical bunches of needle-shaped crystals which either grew directly upon the granular smectite rim or surround nearly spherical cavities,  $2\text{--}5 \mu\text{m}$  in diameter and presumably representing a former alteration product of glass, now dissolved. The needle-shaped phillipsite crystals range, in size, from specimens  $2\text{--}4 \mu\text{m}$  wide and  $8\text{--}12 \mu\text{m}$  long to specimens  $6\text{--}8 \mu\text{m}$  wide and  $15\text{--}25 \mu\text{m}$  long. They show typical prismatic phillipsite morphology, especially the larger ones.

This palisadelike phillipsite is followed by large, stout phillipsite crystals with excellent crystal morphology, up to  $40 \mu\text{m}$  and more in length and width and enclosing several small phillipsite crystals at their bases (Plate 5, Fig. 2). Shards in which stout phillipsite is developed commonly have a hollow interior because the glass or its earlier alteration product has been dissolved. In a few shards this pore space is cemented by calcite, occurring as large, platy, isometric crystals which do not always fill the entire pore. Large calcite may have grown across one or more vesicles whose outlines are still visible by the enclosed smectite rims or fillings (Plate 5, Fig. 2). In a few shards calcite fills only one or several vesicles. Calcite is always intergrown with very small ( $1\text{--}2 \mu\text{m}$ ) elongate or granular crystals of a silicic? mineral visible under crossed polars with the calcite in extinction position by its light grey birefringence. Intergrowth of both phases seems to follow some calcite planes, but is not too well developed. Calcite cement occurs in only a few samples (see Table 1).

These alteration features are restricted to spalling and scoria shards. Alteration of pumice is less complex. In Hole 528, pumice is commonly replaced marginally and around vesicles by cryptocrystalline clay minerals (not necessarily smectite), which in part seem to be oriented tangentially to the surfaces of the shard and the vesicle walls. The interior of pumice shards is generally dissolved. This pore space, as well as primary pore space, may then be cemented by small phillipsite needles and carbonate. Pumice shards of Hole 525A show a distinct alteration history. They are either completely altered to clinoptilolite, that lathlike and platy crystals of which are interspersed through the entire former glass as a chaotic texture (Samples 525A-46-1, 48–55 cm, and 525A-51-2, 95–104 cm). Some clinoptilolite laths show a slightly subparallel arrangement. Vesicles are mostly not preserved, but some shards contain patchy or oval areas of light brown cryptocrystalline clay minerals that could perhaps represent residues of vesicle fillings.

Pumice shards of Core 525A-46, however, are strongly altered to clay minerals. Clay minerals have grown from all walls of the shards, perpendicular to the outside, toward the interior, without leaving any glass. The shapes of vesicles are well preserved by their fillings of cryptocrystalline clay.

#### Lithic Clasts

Lithic clasts are a minor volcanic component in all samples of Hole 528 (Fig. 6) except for some coarse-grained layers where they constitute up to 30 vol.% of the volcanic clasts (e.g., Sample 528-37-1, 135–138 cm, Plate 1, Fig. 2, 528-37-2, 37–40 cm, Plate 1, Fig. 1). In

these layers lithic clasts are predominantly tachylitic to fine-grained, crystalline basalt with varying vesicularity (mostly 5–30%). The tachylite grains vary in shape from very irregular, ragged to rounded forms (Plate 4, Figs. 1, 2; Plate 9, Fig. 1). The ragged, vesicular tachylite that shows partly rounded (fluidal?) edges presumably represents primary clasts produced during the eruption, which should, therefore, have taken place above sea level, where quenching was not so abrupt as it would have been in the water. Some of the tachylite contains euhedral pseudomorphs of olivine and a few glomerophytic aggregates of olivine-pseudomorphs, partly filled with clay minerals along former cracks in the olivine. Single plagioclase crystals and glomerocrysts occur as lathlike phenocrysts within both tachylitic and vitric clasts (Plate 4, Fig. 2; Plate 8, Fig. 1; Plate 9, Fig. 1); they are now mostly replaced by phillipsite and are hollow at the center (see later comments).

Another abundant type of clast is light-colored and contains K-feldspar (rarely plagioclase?) in a fine groundmass that consists of irregularly intergrown feldspar, opaques, and quartz?. Coarser-grained types contain trace amounts of green amphibole intergrown with the groundmass feldspars and opaques. Here, these lithic clasts are called "trachyte," although they are mostly too small to allow exact identification. The grain size of the lithic clasts ranges from <0.1 mm to >2 mm; most are 0.5–1 mm in diameter. Very small amounts of fine-grained (0.1  $\mu\text{m}$ –0.1 mm) "micro-gabbro" clasts are composed of chlorite and some calcite in the groundmass, or feldspar-laths, with some green amphibole. These lithic clasts are present throughout Hole 528. Tachylite dominates in Cores 528-37 and 528-38, whereas "trachyte" is more abundant in the lower Cores 528-41 and 528-46. Samples of 525A are clearly dominated by "trachyte" among the lithic clasts, whereas tachylite is restricted to the lowermost sample (525A-51-2, 95–104 cm).

### Crystal Clasts

Crystal clasts are present in all samples of volcanoclastic rocks, but are generally only a minor component except in the coarse-grained samples. Feldspar occurs in all samples. Fresh plagioclase is extremely rare in samples of both holes. In volcanoclastic rocks of Hole 525A, K-feldspar is most abundant, with only minor plagioclase. The K-feldspar is mostly euhedral sanidine, typically twinned (Karlsbad-twins). Some sanidines reach up to 2 mm in length; most are about 400–600  $\mu\text{m}$  long and nearly as wide (rarely less than 200  $\mu\text{m}$  wide). (Sanidine in Sample 525A-46-1, 48–55 cm is skeletal, presumably because of rapid growth within the melt.) Observations under cathodoluminescence showed that both skeletal and euhedral crystals of all sizes of sanidine illuminated with light to bright blue luminescence, as should be expected for high-T sanidine.

Feldspar crystals from carbonate-free residues of Hole 528 often show a "polished" surface and slightly to well-rounded edges. In these samples most feldspar crystals are in part complexly altered, and it is difficult

to identify them as either K-feldspar or plagioclase (Plate 9). These clasts are totally dissolved; their hollows may be marginally cemented by phillipsite, crystals of which grew nearly perpendicular to the inner surface of the hollows.

Many euhedral (Plate 8) as well as anhedral (Plate 9, Fig. 2) feldspars are surrounded by zeolitized former glass rims, indicating that both types were erupted as phenocrysts. Whereas the anhedral ones could be interpreted as not having crystallized from the melt in whose glass they are now embedded (xenolithic crystal), the euhedral ones, like the one shown in Plate 8, are undoubtedly comagmatic with the surrounding glass. The feldspar of Plate 8 is hollow in some central and marginal areas, has inclusions of brown smectite (former glass?) and marginally and in the interior is replaced by phillipsite. The remaining K-feldspar shows areas with simultaneous extinction and relics of twinning. Although these features indicate that the crystal is a highly altered primary K-feldspar (sanidine?), it does not show any cathodoluminescence.

Other hollow feldspar clasts show margins, connected by ribbons, with simultaneous but in part undulatory and patchy extinction. Toward the hollow interior the feldspar areas are limited by irregular steplike boundaries. Interior parts of hollow-centered feldspar clasts may show small euhedral feldspar with adularia morphology that has generally a round to oval dark core, some smectite, and some unidentified opaque "dust." Some adularia shows simultaneous extinction with the margin of the K-feldspar host. Neither K-feldspar margins nor adularia show any cathodoluminescence. The appearance of adularia-type K-feldspar as euhedral crystals in hollows seems to be clear evidence for the authigenic origin of these crystals, whereas hollow-centered feldspar appears to be a relic structure of primary feldspar. Kelts and McKenzie (1976) have interpreted similar features of K-feldspar in volcanogenic sands along the Line Chain, in the Pacific, to be the result of diagenesis. A similar interpretation of nonluminescent feldspars is proposed by Kastner (1977; Kastner and Siever, 1979). Kelts and McKenzie (1976) suggest that a combination of "pseudomorphic replacement of plagioclase or other feldspar" and precipitation of K-feldspar "directly from a hydrothermal solution filling the voids and replacing the matrix" is responsible for the formation of the features observed in the K-feldspar.

Spinel and clinopyroxene are rare and are restricted to Hole 528 samples. Carbonate-free residues of volcanoclastic rocks in Hole 528 (e.g., 528-37-2, 37–40 cm, and 528-37-3, 18–20 cm) contain single grains of green augite of more than 500  $\mu\text{m}$   $\phi$ . Most augite appears fresh in thin section and grain mounts, but the terminations of crystals show coxcomb dissolution features. Intrastatal solution of clinopyroxene is supported by textural evidence in thin section, where the hacksaw-terminated crystals seem to lie in a cavity within the groundmass. Minor amphibole appears in Hole 525A samples. It is correlated with the occurrence of amphibole-bearing lithic clasts.

### Nonvolcanic Clasts

There are two kinds of nonvolcanic clasts in the volcanoclastic rocks studied: biogenic clasts (fragments or whole skeletons of mostly calcareous fossils) and intraclasts or lumps of ooze. Foraminifers dominate the biogenic clasts, but fragments of bryozoans, coralline algae, molluscan shells, and echinidae are also present in a few samples. These fragments of mostly typical shallow-water fossils do not occur in all samples but are present throughout the entire studied section of Hole 528 and in the lowermost sample of Hole 525A. The upper parts of volcanoclastic units may be enriched in foraminifers, but they are often accumulated in distinct layers 1 to 3 mm thick in the middle or lower part of a volcanoclastic unit. The chambers of most foraminifers are filled with greenish or mostly brownish clay (glauconite?). These fillings remain untouched after carbonate dissolution and thus are a main component of the 63–125  $\mu\text{m}$  fractions of a few samples. Some of the foraminifers show carbonate cement grown perpendicular to the surface. The dark brown rim surrounding the cement suggests that this must have grown before the shells were embedded in the volcanoclastic unit. Broken foraminifers which show that the cement existed before the foraminifers broke are evidence for re-sedimentation of these shells.

Nonbiogenic, nonvolcanic clasts are intraclastlike lumps of ooze, generally elliptic, occurring mainly in the basal parts of volcanoclastic units but also found in the upper parts. They cannot always be clearly separated from burrows, which are very abundant in the upper parts of volcanoclastic layers (see site reports, this volume). These "intraclasts" range in size from 150 to >2000  $\mu\text{m}$ .

### Groundmass

Most clasts are embedded in a light to dark brown clayey groundmass; grain-supported framework is uncommon, but may occur in the middle parts of volcanoclastic layers. Marly groundmass is mostly restricted to the bottom or top of volcanoclastic layers and may represent inworked nannofossil ooze. The upper parts of clastic units are sometimes strongly bioturbated, a process during which overlying calcareous sediment may be admixed into the volcanoclastic material. Carbonate ooze has also been taken up and inworked into the lower parts during transport of the mass flow (probably as a turbidity current).

The clayey groundmass is often composed of small spherical aggregates of 3–8  $\mu\text{m}$   $\phi$ . Clasts are mostly surrounded by a dark rim of this material, which partly levels the roughness of the clasts by filling inlets on the grain's outer surface. Extremely thin parts of thin sections show the groundmass to consist of light brown grains, generally far less than 1  $\mu\text{m}$   $\phi$ . XRD analyses of the <2  $\mu\text{m}$  fractions of carbonate-free residues of these samples (see later) show smectite as the only crystalline phase. Thus, at least part of the matrix may be altered vitric ash.

Some of the smectite in the groundmass may be due to alteration of the larger shards, whereby material cre-

ated through dissolution of shards was moved into primary pore space and precipitated as small granular or bladed smectite. The latter is mostly developed in matrix-free or matrix-poor samples (e.g., the lowermost thin layer of the volcanoclastic sediment of Sample 528-37-7, 42–46 cm, Plate 2, Fig. 2). The remaining interparticle pore space is subsequently chiefly cemented by phillipsite in Hole 528 samples and by clinoptilolite in Hole 525A samples (Plate 6, Fig. 2).

### Microscopic Textures of Volcanoclastic Rocks and Occurrences of the Volcanic Components throughout Holes 525A and 528

#### Hole 525A

Volcanoclastic rocks in Hole 525A are quite different from those in Hole 528, both in texture and composition. In Hole 528, as already noted, they form distinct layers. The four samples studied from Hole 525A are nannofossil oozes rich in volcanic particles. In three samples (525A-46-1, 48–55 cm, 525A-46-4, 42–45 cm, and 525A-46-4, 45–53 cm), the volcanoclastic material occurs enriched in lenses and dispersed within the ooze, whereas in Sample 525A-51-2, 95–104 cm it forms a distinct layer. True volcanoclastic rocks may be present in this hole as well (see site report, this volume), but no samples of these rocks were obtained.

The lowermost sample of Hole 525 (525A-51-2, 95–104 cm) contains a polymictic volcanogenic assemblage, consisting mainly of feldspar clasts (K-feldspar and plagioclase) and pumice lapilli that are now totally altered to clinoptilolite. Minor, vesicle-free sideromelane shards occur as well as "palagonitized" shards which are obviously broken after "palagonitization." A few vesicular tachylite lapilli are present. These clasts range in size from 60 to 200  $\mu\text{m}$  and are enriched in a nearly matrix-free, well-sorted layer.

Nonvolcanic clasts of this sample constitute over 30 vol.% and are fragments of shallow-water fossils such as bryozoans, coralline algae, and molluscs (among them abundant calcite prisms of *Inoceramus*), with fewer foraminifers. Platy clinoptilolite occurs as interparticle cement (Plate 6, Fig. 2) and filling of foraminiferal chambers. A few elongated and cryptocrystalline calcite structures could represent calcite-cemented pumice clasts. Large calcite crystals partly cement pore spaces between particles.

Volcanic clasts of this layer are clearly epiclastic, although some of them are of pyroclastic origin (pumice and tachylite lapilli). The sediment and part of the surrounding nannofossil ooze are interpreted as the product of slumping or turbidity current deposit. The lack of any obvious bedding structure favors the interpretation that they are small-scale slumping deposits.

In the three samples from Core 525A-46, the volcanic components are very similar. In Samples 525A-46-4, 42–45 cm and 525-46-4, 45–53 cm, the volcanic particles are mainly lithic clasts of "trachyte" (up to 2 mm  $\phi$ ) and sandine (up to 1 mm long). Some trachytes have enclosed sandine phenocrysts. Minor pumice shards are totally altered to clay minerals, as already noted. Vol-

canic clasts of more basaltic composition are nearly absent, except for a very few tachylite fragments in Sample 525A-46-4, 42–45 cm. Volcanic clasts are dispersed within the groundmass of nannofossil ooze, sometimes slightly enriched in lenses. Nonvolcanic clasts of these samples consist of rare foraminifers. The uppermost sample of this hole (525A-46-1, 48–55 cm) contains some clasts of trachyte?, dispersed in a matrix of calcareous ooze, many euhedral sanidines, partly corroded, and pumice clasts that are now totally altered to clay minerals and clinoptilolite. These pumice clasts are macroscopically developed as green, irregularly shaped clasts similar to those of 525A-46-4, 55–53 cm (Plate 1, Fig. 5). A few crystals of brown and green amphibole are scattered through this sample. All volcanic components may be "trachytic," in a broad sense. Nonvolcanic clasts, as in the other samples of Core 525A-46, consist of sparse foraminifers.

### Hole 528

As already described, three volcanoclastic units were cored in the lower part of Hole 528 (Cores 37–46; see Fig. 4). The lower one, intercalated within basement, comprises at least six distinct volcanoclastic layers of more than 10 cm thickness, and some thinner layers.

Samples of three layers show from Sections 528-41-1, 528-43-1, 528-46-2 (one sample each) three different compositions. The lowermost sample, from 539 m sub-bottom depth (528-46-2, 107–110 cm) is dominated by pumice, altered to clay minerals, and clasts of K-feldspar embedded together with abundant foraminifers in a matrix of ooze. Calcite prisms of *Inoceramus* are common. This layer, probably of turbidity-current origin, compositionally resembles most layers of Hole 525A.

The next sample, taken 29 m higher in the hole (528-43-1, 23–26 cm), is of quite different composition, with abundant, highly altered, vesicular scoria shards, strongly altered, hollow-centered feldspar clasts, some with former glassy rims, and lithic clasts of fine-grained basalt. These clasts are embedded in a matrix of relics of fine-grained spalling shards and smectite. Nonvolcanic clasts are nearly absent, except for a very few foraminifers.

Another volcanoclastic layer of strongly altered pumice shard tuff with only very few feldspar clasts and fewer foraminifers, probably of turbidite origin, was cored 18 m higher (528-41-1, 57–61 cm). Horizontal bedding is well developed and may have been accentuated by compaction of the elongate pumice shards.

The second and third units of volcanoclastic sediments begin in Core 528-38 and extend nearly to the top of Core 528-37. From 454.5 to 464 m sub-bottom (Core 37) more than 10 distinct volcanoclastic layers were cored. These are, insofar as they have been studied (compare sample location in Fig. 3), rather uniform in general composition but different in texture, mostly because of differences in grain size, and (depending on the grain sizes of the clasts) contain varying amounts of the three types of volcanic clasts. Volcanoclastic rocks with clasts of coarse sand size (or larger) contain generally more lithic and crystal clasts than fine-grained layers (fine

sand to silt). Vitric clasts of Core 37 are mainly scoria and spalling shards, with subordinate pumice. Shards are always strongly altered, so that the distinction between scoria and pumice is sometimes quite uncertain. Tachylite and lesser amounts of fine-grained basalt dominate among the lithic clasts of the Core 37 volcanoclastic rocks. Tachylite is often vesicular, with residues of feldspar and olivine pseudomorphs; plagioclase microlites are rare. Ragged clast outlines are common for tachylite; they are interpreted as evidence of pyroclastic origin. Tachylite occurs throughout all samples from the volcanoclastic rocks of Core 37 and is enriched in coarse-grained layers.

### XRD STUDIES OF VOLCANICLASTIC ROCKS

XRD analyses were made of whole rock samples of the volcanoclastic layers and of part of the nannofossil-ooze samples (Table 2). The oozes are very uniform in mineralogy, consisting dominantly of calcite, quartz, small amounts of mica and smectite, and less feldspar. X-ray amorphous material is present throughout all samples, causing a weak broad hump of the background between  $18^\circ$  and  $36^\circ 2\theta$ . Only one sample of nannofossil ooze (528-37-4, 119–123 cm), which lies 0.5 to 1 cm below a strongly zeolitized volcanoclastic layer, contains some phillipsite, whereas all other samples of ooze are free of zeolitic minerals. Similarly, at Sites 397 and 398 (Leg 47), Riech (1979) failed to find zeolites in the immediate vicinity of ash layers.

The volcanoclastic rocks of Holes 528 and 525A show major differences both in primary and secondary mineralogy. The main volcanogenic mineral in samples from Hole 525A is a high-T sanidine. Alteration minerals of these samples are clinoptilolite and smectite. The microscopic identification of clinoptilolite rather than heulandite was verified by heating the powdered samples for 15 hr. at  $350^\circ\text{C}$  and, after 30 min. of cooling, X-raying again. During this procedure, heulandite is destroyed to an X-ray amorphous state but clinoptilolite remains nearly untouched (Mumpton, 1960; Alietti, 1972; Boles, 1972).

Samples from Hole 528 contain only minor feldspar, which cannot be exactly determined in whole rock samples, mostly because the peaks are overlain by strong phillipsite lines. All volcanoclastic rocks of Hole 528 contain phillipsite and smectite as dominant alteration minerals. K-feldspar and thomsonite?, which are present in thin sections, cannot be identified in X-ray diagrams because they appear in only trace amounts.

Insoluble residues of a few samples of volcanoclastic rocks were obtained (Table 3). The  $2\ \mu\text{m}$  fraction of all these samples is clearly dominated by smectite with only minor amounts of X-ray amorphous material. The position of the basal reflection (001) of these smectites lies between 12 and  $13.5\ \text{\AA}$  for air-dried samples and swells to  $16.9\text{--}17\ \text{\AA}$  after 24 hr. of glycolization (at  $50^\circ\text{C}$  in a drying stove). The morphology of the (001)-reflex of the glycolization samples and the ratio of the height above background at  $5.1^\circ 2\theta$  versus height at  $4^\circ 2\theta$  can be taken as evidence of the type and degree of interstratification of smectite mixed-layer minerals (Reynolds and Hower,

Table 2. Qualitative results of whole rock XRD analyses, Holes 525A and 528.

Sample (interval in cm)	Minerals								Rock Type
	Smectite	Mica	Calcite	Quartz	Sanidine	Feldspar (undifferentiated)	Clinoptilolite	Phillipsite	Volcaniclastic Rock Ooze with Ooze
<b>525A</b>									
46-1, 48-55	A	P	A	P	D		A		A
46-4, 45-53	A		D	P	D				A
51-2, 95-104	P	P	D	P	D		A		A
<b>528</b>									
37-1, 49-51	P	P	A	?		P	D	A	
37-1, 95-98	A	P	o	P		P	A	A	
37-1, 135-138	P	P	A	A		A			A
37-1, 135-138	A	P	P	A		A	D	A	
37-1, 141-142		P	D	A					A
37-2, 34-37	A		D	-		A	A	A	
37-2, 37-40	P	P	A				D	A	
37-2, 50-52	P		P	P		P	D	A	
37-2, 61-64	A	P	A			P	D	A	
37-2, 80-82	A	P	P	P			D	A	
37-2, 97-101	P	P	o	P			A	A	
37-2, 119-123	A	P	A	P			D	A	
37-2, 148-150	A	A	A	P			D	A	
37-3, 8-11	A	P	A			P	D	A	
37-3, 18-20	A	P	P	P		P	D	A	
37-4, 111-114	A	P	A	P		P	D	A	
37-4, 119-123	P	P	D	P			A		A
37-4, 119-123	A	P	A	P		P	D	A	
37-6, 117-120	P	P	A	P			D	A	
37-6, 129-132	A		A	P		P	D	A	
37-6, 140-143	A		A	P		P	D	A	
37-6, 147-150	A		A	P		P	D	A	
37-7, 14-17	A		A	P		P	D	A	
37-7, 17-20	A		A	P		P	D	A	
37-7, 20-23	A	A	D	A				A	
37-7, 23-27	A	P	D	A					A
37-7, 27-37	A	P	D	A					A
37-7, 31-35	A	P	P	P		P	D	A	
37-7, 42-46	A	P	D	A		P	?		A
37-7, 42-46	A	P	P	P		P	D	A	
38-2, 64-65	A	P	D	A		P			A
38-3, 68-69	A	P	D	A		P			A
38-4, 90-92	A	P	D	A		P			A
41-1, 57-61	A		A	:		P	D	A	
43-1, 105-106	A	P	D	A		P			A
44-1, 66-67	A	P	D	A					A
46-2, 48-50		A	D	A					A
46-2, 107-110	P	A	D	A		P			A
46-2, 107-110	P		A	A		D	D	A	

Note: D = dominant, A = abundant, P = present.

1970). Comparison of our samples with tables of defined mixed-layer minerals of random interstratification (Reynolds and Hower, 1970) shows the smectites of most samples to be free of interstratified nonexpandable

Table 3. Insoluble residues of volcanoclastic rocks, Holes 525A and 528.

Sample (interval in cm)	Insoluble Residue (wt.%)	Total Residue (wt.%)			
		<2 $\mu\text{m}$	2-63 $\mu\text{m}$	63-250 $\mu\text{m}$	>250 $\mu\text{m}$
<b>525A</b>					
46-1, 48-55	53.4	51.3	44.5	3.2	1.0
46-4, 45-53	63.7	21.5	52.9	9.5	16.1
<b>528</b>					
37-1, 95-98	75.0	22.2	41.1	35.6	1.1
37-2, 37-40,b	75.5	14.5	26.5	27.7	31.3
37-2, 61-64	59.2	20.4	70.6	9.1	0.9
37-2, 119-123	81.6	13.3	43.4	42.8	0.5
37-3, 18-20	66.7	9.5	27.8	55.7	7.0
37-4, 111-114	74.9	14.7	50.6	34.3	0.4
37-4, 119-123	79.6	11.7	53.4	32.3	2.6
37-6, 140-143	76.5	17.1	43.2	36.7	3.0
37-6, 147-150	79.5	17.3	47.6	29.8	5.3
37-7, 35-42	78.3	13.0	34.0	52.4	0.6
37-7, 42-46	81.7	14.1	39.9	42.6	3.4
41-1, 57-61	79.4	16.0	61.1	22.1	0.8
46-2, 107-110	75.2	25.2	56.3	17.5	1.0

Note: Insoluble residues are carbonate-free and free of organic matter. Since samples obtained were small (4-6 g), grain-size distributions are not representative. Primary grain-sizes of glass shards were destroyed by intense alteration.

layers. The (060)-reflex of smectite, which is about 1.5 Å for dioctahedral (Al) and 1.53 Å for trioctahedral (Mg) smectites, is not well developed in these samples, which cannot be obtained free of texture and shows that all samples contain a mixture of tri- and dioctahedral smectites in which the trioctahedral component seems to be dominant.

Smectite is present in all grain-size fractions, in coarser fractions (up to 63  $\mu\text{m}$ ), as diagenetic margins in and around former glass shards (now zeolitized and broken into zeolitic aggregates with rims and inclusions of smectite) and lithic fragments, as inclusions in larger phillipsite crystals and K-feldspar, and as small, indurated aggregates which are not destroyed during ultrasonic treatment.

### BULK ROCK CHEMICAL COMPOSITION

Thirteen whole rock samples were analyzed for major elements and for 10 trace elements (Table 4; Figs. 7, 8). From Hole 525A, only one sample appeared homogeneous enough to be analyzed chemically. Most rocks have about 5 to 7%  $\text{H}_2\text{O}^+$  and from 1 to 4%  $\text{CO}_2$ . These high  $\text{H}_2\text{O}^+$  and  $\text{CO}_2$  contents and the high  $\text{Fe}_2\text{O}_3/\text{FeO}$  ratios (mostly > 1) indicate significant alteration in the rocks, which is to be expected from the dominantly glassy primary composition. Table 4 contains analyses recalculated  $\text{H}_2\text{O}$ -free, not  $\text{CO}_2$ -free, since to include  $\text{CO}_2$ -free analyses would result in overcorrection in many cases, indicating that a significant portion of the Ca combined in calcite (Mg-poor or Mg-free) is derived from the system itself. (Two exceptions, Samples 525A-51-2, 95-104 cm and 528-37-1, 95-98 cm, contain abundant carbonate fossil debris.) We discuss alteration changes elsewhere in more detail; here we list only some of the main chemical features. Although many of the basement lavas analyzed by Richardson et al. (this volume) are also altered, they provide a more homogeneous data set and allow some general conclusions.

Table 4. Whole rock chemical analyses (XRF) of volcanoclastic sediments from Holes 525A and 528.

Element	525A-51-2, 95-104 cm *	528-37-1, 95-98 cm *	528-37-2, 34-37 cm *	528-37-2, 119-123 cm *	528-37-2, 148-150 cm *	528-37-3, 8-11 cm *	528-37-4, 111-114 cm *	528-37-6, 129-132 cm *	528-37-6, 140-143 cm *	528-37-7, 14-17 cm *	528-37-7, 35-42 cm *	528-41-1, 41-1, 57-61 cm *	528-46-2, 107-110 cm *													
Major element oxides (wt.%)																										
SiO <sub>2</sub>	42.5	43.9	41.6	44.3	45.2	48.3	47.0	49.99	44.7	47.38	47.6	50.36	43.6	46.45	49.0	51.96	47.8	51.3	49.4	52.29	49.7	53.06	49.4	52.61	51.8	55.99
TiO <sub>2</sub>	1.82	1.88	1.84	1.96	2.09	2.23	2.06	2.19	1.94	2.06	1.92	2.03	2.02	2.15	1.86	1.97	1.86	2.0	1.91	2.02	2.32	2.48	1.59	1.7	0.85	0.92
Al <sub>2</sub> O <sub>3</sub>	13.92	14.38	12.97	13.81	15.48	16.54	15.76	16.76	14.98	15.88	16.26	17.2	14.76	15.72	16.12	17.09	15.59	16.73	16.59	17.56	16.5	17.61	15.27	16.29	13.28	14.35
Fe <sub>2</sub> O <sub>3</sub>	3.74		5.33		6.61		4.92		5.49		5.37		4.79		4.42		5.15		4.09		4.12		4.65		4.22	
FeO*	4.58			9.29		11.31		9.5		9.74		9.14		9.84		7.66		9.52		8.06		7.64		5.54		5.03
FeO	1.06		3.92		4.63		4.5		4.25		3.81		4.93		3.24		4.24		3.93		3.45		0.98		0.85	
MnO	0.07	0.07	0.3	0.32	0.15	0.16	0.13	0.14	0.14	0.15	0.12	0.13	0.16	0.17	0.09	0.1	0.12	0.13	0.1	0.11	0.08	0.09	0.07	0.07	0.08	0.09
MgO	1.44	1.49	6.53	6.95	7.52	8.04	7.0	7.45	7.86	8.33	6.9	7.3	6.84	7.29	5.82	6.17	7.46	8.01	6.08	6.44	5.1	5.44	3.35	3.57	2.6	2.81
CaO	16.44	16.98	9.58	10.2	2.7	2.89	3.39	3.61	4.74	5.02	3.29	3.48	6.06	6.46	3.74	3.97	2.86	3.07	2.8	2.96	2.78	2.97	6.14	6.55	7.07	7.64
Na <sub>2</sub> O	2.64	2.73	2.94	3.13	3.56	3.8	3.9	4.15	3.74	3.96	4.22	4.46	3.28	3.49	3.97	4.21	3.63	3.9	3.89	4.12	4.2	4.48	4.62	4.93	4.44	4.8
K <sub>2</sub> O	2.22	2.29	1.87	1.99	2.16	2.31	2.89	3.07	2.26	2.4	2.54	2.69	2.63	2.8	3.57	3.79	2.97	3.19	3.61	3.82	3.74	3.99	3.22	3.44	2.93	3.17
P <sub>2</sub> O <sub>5</sub>	0.3	0.31	0.37	0.39	0.3	0.32	0.39	0.41	0.38	0.4	0.35	0.37	0.3	0.32	0.15	0.16	0.21	0.23	0.09	0.1	0.11	0.12	0.11	0.12	0.11	0.12
H <sub>2</sub> O <sup>+</sup>	2.66		5.26		6.98		6.17		6.11		6.15		6.6		6.16		5.79		6.01		6.0		6.25		6.44	
CO <sub>2</sub>	10.61	10.96	6.73	7.17	3.46	3.7	2.13	2.27	4.11	4.36	2.24	2.37	4.65	4.95	2.28	2.42	1.42	1.52	2.0	2.12	1.52	1.67	4.46	4.76	4.41	4.77
Total	99.42		99.2		100.84		100.24		100.13		100.57		100.62		100.42		99.1		100.5		99.66		100.11		99.08	
Minor elements (ppm)																										
S	0.08	0.08	0.05	0.05	0.03	0.03	0.04	0.04	0.03	0.03	0.05	0.05	0.03	0.03	0.05	0.05	0.04	0.04	0.03	0.03	0.03	0.03	0.03	0.03	0.04	0.04
Cl	0.16	0.17	0.3	0.32	0.22	0.24	0.28	0.3	0.16	0.17	0.26	0.28	0.17	0.18	0.31	0.33	0.23	0.25	0.24	0.25	0.24	0.26	0.08	0.09	0.05	0.05
Cr	46	47	47	50	61	65	81	86	77	81	93	98	75	79	93	98	96	103	99	104	77	82	54	57	19	20
Ni	30	30	60	63	53	56	42	44	51	54	51	53	80	85	78	82	78	83	58	61	38	40	30	32	25	27
Cu	14	14	79	84	60	64	66	70	92	97	63	66	173	184	130	137	183	196	125	132	77	82	48	51	28	30
Zn	44	45	105	111	104	111	95	101	91	96	93	98	123	131	97	102	106	113	80	84	78	83	118	125	174	188
Rb	54	55	27	28	32	34	38	40	38	40	35	37	37	39	47	49	42	45	46	58	58	61	55	58	66	71
Sr	725	748	239	254	223	238	219	232	243	257	225	238	269	286	235	249	216	231	217	229	214	228	227	242	370	399
Y	24	24	31	33	29	30	32	34	30	31	29	30	26	27	23	24	27	28	18	19	21	22	34	36	87	94
Zr	187	193	191	203	223	238	216	229	207	219	199	210	214	227	167	117	155	166	164	173	203	216	423	451	757	818
Nb	30	30	38	40	47	50	44	46	42	44	39	41	40	42	31	32	30	32	33	34	41	43	83	88	114	123
Ba	622	642	132	140	299	319	376	399	270	286	421	445	304	323	355	376	318	341	342	362	697	744	863	920	425	459
Total	99.84		99.68		101.2		100.68		101.0		101.2		100.95		100.91		99.5		100.89		100.08		100.41		99.38	

Note: Values in columns marked with asterisk are H<sub>2</sub>O-free.

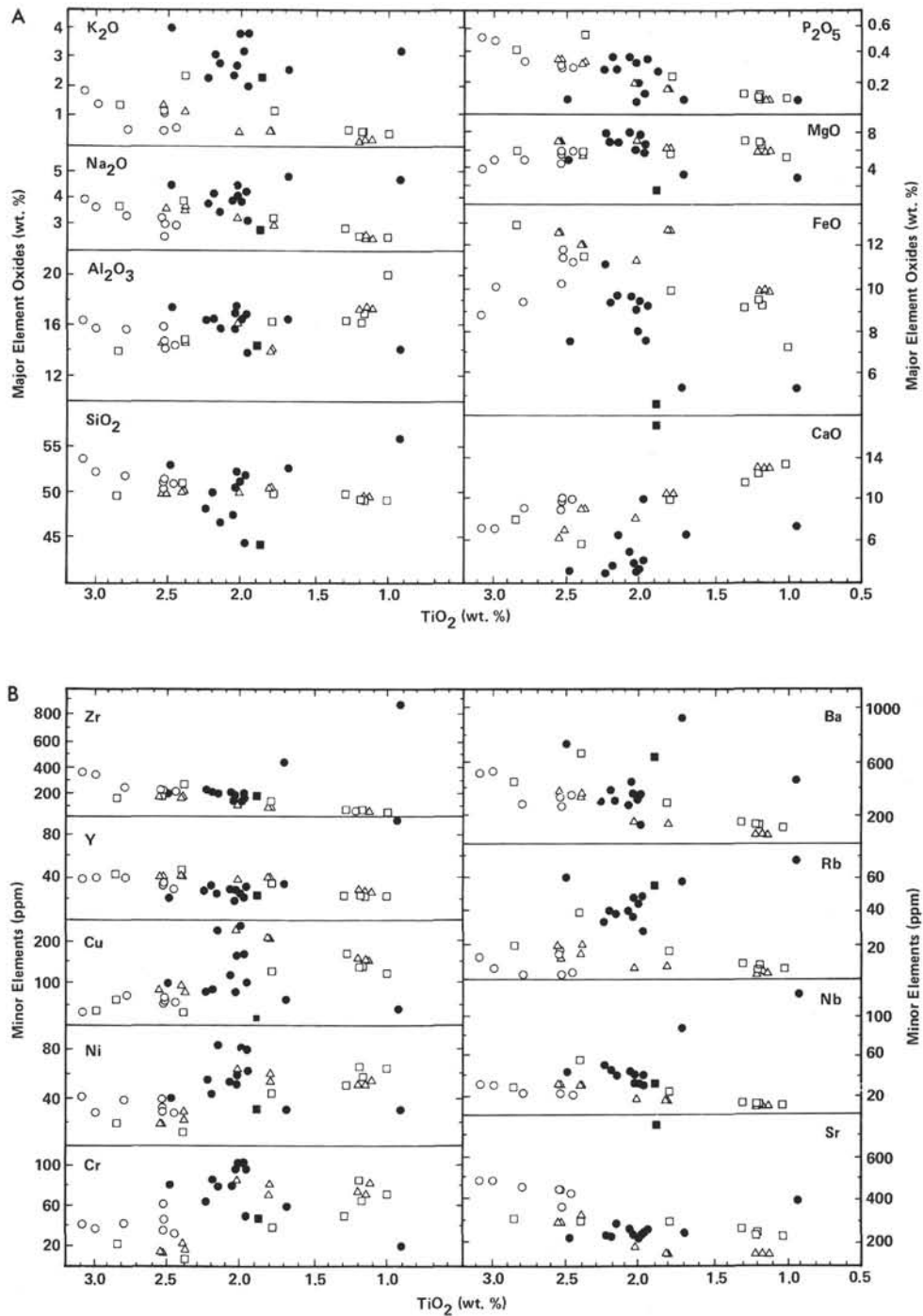


Figure 7. TiO<sub>2</sub> variations in basalts and volcaniclastic rocks. XRF whole rock analyses of (A) major elements and (B) trace elements. Open symbols indicate basalts, analyzed by Richardson et al. (this volume); solid symbols indicate volcaniclastic rocks. Circles = Hole 525A, triangles = Hole 527, squares = Hole 528.

Volatile-free analyses are clearly basaltic in composition, with most elements departing remarkably little from (evolved) basalts, despite the very extensive and complex alteration history already described. This is true not only for relatively immobile elements such as Ti but also for MgO, Al<sub>2</sub>O<sub>3</sub>, and Na<sub>2</sub>O, in part. In some samples SiO<sub>2</sub> is enriched relative to TiO<sub>2</sub>; in other samples, it is depleted. The most striking changes are the

massive depletion in Fe and Ca and the drastic increase in K among the major elements, and the increase in Rb among the trace elements. Judging from the concentrations of compatible trace elements such as Cr and Ni, the basalts are all fractionated; this interpretation is in accordance with the mineralogical observation. Even though the volcaniclastic flows are likely to be derived from seamounts and islands, the composition of the ba-

## DISCUSSION

Volcanic clasts in deep sea sediments can have very different origins. They can form nearby *in situ*, for example, by spalling of glassy pillow margins or flow tops, at lower hydrostatic pressures such as in high-standing seamounts, or subaerially on volcanic islands. Tephra produced in shallow water or on land may become abraded and mixed with other clasts during transport, except for clasts produced close to the site of deposition or fallout tephra from Plinian eruption columns. Volcanic clasts produced entirely by erosion of pyroclastic or other volcanic rocks, in very shallow water or on land, will show especially wide ranges in composition, texture, and degree of abrasion.

Although vitric clasts are dominant in the volcanoclastic rocks from Holes 525A and 528, their composition is inferred chiefly from that of phenocrysts as well as from cogenetic lithic and crystal clasts, because the glass shards are much more strongly altered than the lithic and most of the crystal clasts. Most vitric shards of Hole 528 are classified as scoria by their morphological appearance—a classification which implies a basaltic to intermediate composition. Pumice is mostly restricted to the lower part of Hole 528 and to Hole 525A. Thus glass shard residues and lithic clasts and their phenocrysts indicate that the composition of the source area ranges over a wide spectrum, from olivine-phyric basalts (dominantly in Hole 528) to highly differentiated (trachytic or rhyolitic?) compositions (lower part of 528, 525A). Most common in Hole 528 samples are aphyric to plagioclase-phyric basalts. Most significant is the scarcity of clinopyroxene phenocrysts, which in island-derived deep sea volcanoclastics are generally not only most common but also most resistant to alteration (e.g., Schmincke and von Rad, 1979). The clinopyroxenes are slightly affected by intratratal solution, as the presence of coxcomb terminations indicates, but the scarcity of hollows which could represent former pyroxenes destroyed by dissolution suggests that the paucity of clinopyroxene is real. Most probably the source magmas were dominantly plagioclase and olivine-phyric tholeiites such as in Iceland, and not true alkali basalts such as are common in most oceanic islands. By this line of reasoning, the highly differentiated rocks most likely represent trachyte rather than phonolite-type derivative magmas. In either case, the mere occurrence of abundant, differentiated rocks is evidence for a volcano system that had evolved beyond the shield stage and had developed high-level magma chambers in which highly evolved magmas could originate. The abundance of sanidine in Hole 525A is evidence for a fairly high level of K-enrichment, a geochemical signature of the volcanic islands of the Tristan group and Gough Island (Le-Maitre, 1962; Baker et al., 1964).

It is difficult to specify the water depth of volcanic activity except in most general terms. The fact that vesicular tachylite occurs as the primary volcanic clast throughout the section at Hole 528 and at the base of Hole 525A suggests that subaerial volcanism was active

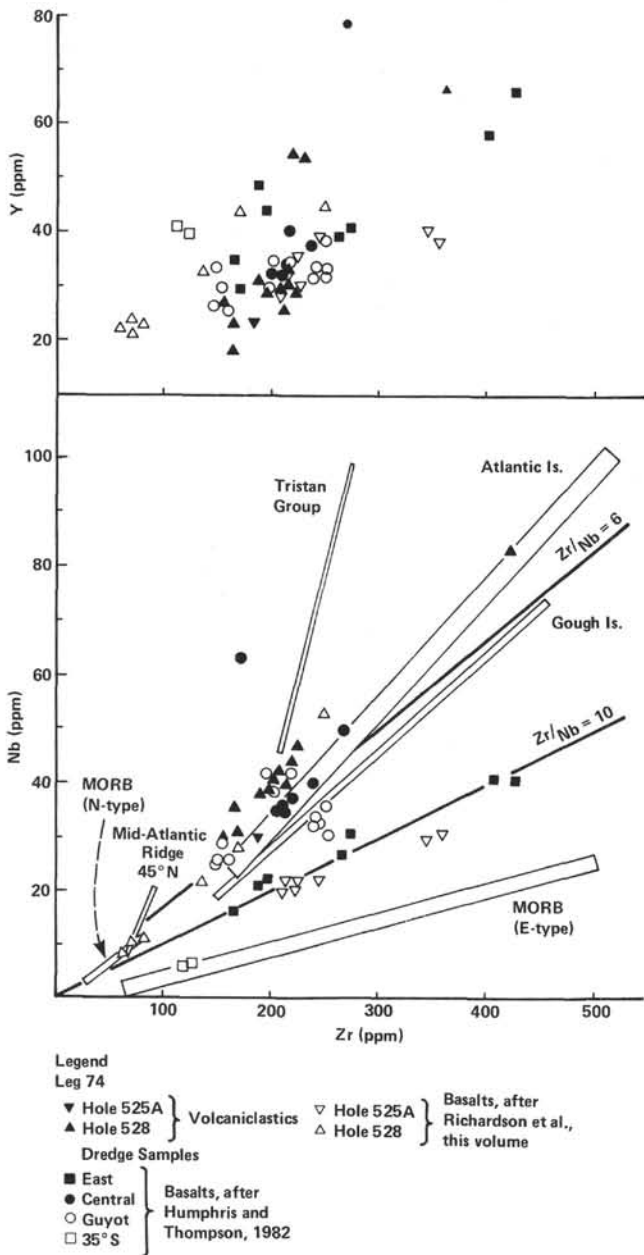


Figure 8. Zr/Nb and Zr/Y ratios of volcanoclastic sediments and basalts from the Walvis Ridge. Trends of Zr/Nb ratios of basalts from different oceanic environments are shown for comparison (after Richardson et al., this volume); width of trend lines is proportional to the scattering of points belonging to each field.

saltic volcanoclastic rocks essentially resembles those of the basement basalts analyzed by Richardson et al. (this volume) in the two main, characteristic features: (a) Many of the basalts are more fractionated than "average" MORB and (b) the basalts are enriched in incompatible elements compared to "normal" MORB. The sample from Hole 525A as well as the two "trachytic" samples from Hole 528 (528-41-1, 57-61 cm, 528-46-2, 107-110 cm) are more fractionated, as expected, but only one of these "trachytic" samples is depleted in compatible elements (Sample 528-46-2, 107-110 cm).

at the time the lowermost volcanoclastic rocks were formed (Campanian–Maestrichtian). On the other hand, the abundance of nonvesicular to highly vesicular (former) sideromelane shards is highly suggestive of abundant, shallow-water, submarine explosive eruptions, probably at water depths of a few tens to a few hundreds of meters. In basalts sampled across the Reykjanes Ridge at varying water depths, vesicularity increases strongly in the upper 500 m (Moore and Schilling, 1973). The seamount section of La Palma, Canary Islands, shows a drastic increase in vesicularity in the tephra clasts in the upper 700 m (Staudigel and Schmincke, unpublished data). The mingling of vesicular tachylite with sideromelane shards could indicate either contemporaneous, shallow, submarine and subaerial volcanism at one or more sources or mixing of these clasts on the submarine slope of a volcano before second-stage transport by some kind of mass flow occurred. Mass flows may have resulted when rapidly accumulated piles of sideromelane ash and lapilli episodically “slumped” off the upper slope of one or more volcanoes, possibly triggered by continuing vulcano–tectonic events in the growing seamount or island.

The pumice shards, on the other hand, are probably derived from large, Plinian eruptions during the late stage in the evolution of an island. Their dominance at the base of 525A and in the lowermost parts of 528 (Samples 528-41-1, 57–61 cm and 528-46-2, 107–110 cm) may indicate that at the time they were deposited (Maestrichtian) different island stages coexisted in the area of the Walvis Ridge and contributed material to deep marine sedimentation. In this part of Hole 528 (Cores 37–47), the ooze and volcanoclastics are interlayered within basalt flows (and pillows?), indicating great proximity to a mid-ocean ridge. Thus, the volcanoclastic sedimentation history of Hole 528 occurred in two stages: first came both tephra fallout and mass flow deposits from at least two different sources, followed by dominance of mass flow sedimentation originating from submarine slopes of volcanic islands and seamounts.

What can we infer about the duration of seamount and island volcanism? In Hole 525A, the top of basement is about 70 m.y. old (see site report, this volume), and volcanoclastic sedimentation started as lava extrusion waned. Volcanic rocks are found here up to the middle Maestrichtian (~66–68 Ma). Thus volcanoclastic sedimentation lasted about 2 m.y. (up to 105 m above basement). At Site 528, volcanoclastic sedimentation was episodic, with the first phase older than the top of basement (68–70 m.y.). Two further episodes of volcanoclastic sedimentation continued to about  $5 \times 10^5$  y. after basement volcanic activity ended.

The geographic location of the source area of the volcanoclastic sediments can be deduced from shipboard reports of the Walvis Ridge transect sites. At Site 524, Leg 73, which was situated southeast of the Ridge at a present water depth of 4796 m (Fig. 1), sediments of Maestrichtian age contain abundant volcanoclastic layers, mostly 10 to 30 cm and up to 80 cm thick, interlayered with beds of ooze 10 to 50 cm thick. The volcanoclastic sediments, interpreted as turbidity current deposits,

make up about 40–50% of the sediments in the lower 60 m of this hole. The southeast of the Walvis Ridge is extremely steep, a morphological feature dating back to the Late Cretaceous, as is indicated by the occurrence of thin volcanoclastic turbidites. Thus it did not allow the accumulation of great piles of volcanic pyroclastic material, which soon after its first deposition was transported toward the basin. The volcanic source of the Hole 524 volcanoclasts must have been situated somewhere on the ridge itself; it was probably the same as the source for the volcanoclastic rocks of Leg 74. The five main sites of Leg 74 are situated at present water depths of between 1054 and 4428 m, and the cored sediments show that the morphological situation was similar during the Late Cretaceous, when the highest point (Site 526) lay in the southeast part of the transect. According to the shipboard party, which relied upon a lithosphere cooling or “backtracking” technique in combination with the oldest fossils recovered (represented by shallow-water biocalcarenes), this highest point did not sink below sea level until the late Paleocene. The deepest site (527) lay at that time in a water depth of about 2200 m (see site reports, this volume). Water depths in the Late Cretaceous, a time of high volcanoclastic production and the last phase of basement volcanism, were shallower: a few hundred meters at Site 525, about 1500 m at Site 528, and more than 2200 m at the deepest Site 527 (shipboard party results, estimated mostly by benthic microfossils). The volcanoclastic interval of Leg 74 is thickest at Site 525, closest to the crest of the Walvis Ridge, and becomes progressively thinner toward the northwestern basin sites, with only dispersed volcanic material in the deepest site. Thus all data point toward the Walvis Ridge itself as the main source of the volcanic material. The Ridge itself was perhaps a chain of seamounts and volcanic islands throughout Late Cretaceous time.

Diagenetic changes in the volcanoclastic rocks reflect their primary composition and changes in pore solution chemistry, porosity, and permeability. Volcanoclastic rocks from Holes 525A and 528 differ strongly in their primary composition: those of 525A are generally more siliceous. These samples contain, as an alteration product of volcanic glass, abundant, small clinoptilolite crystals, scattered throughout primary pore space. Felty clinoptilolite laths replace pumice, which at the margins as the first step of alteration, is replaced by clay minerals (smectite and illite?). In the generally more basaltic samples of Hole 528, phillipsite is the main diagenetic mineral together with abundant smectite, crystals of which may reach considerable sizes (10  $\mu$ m).

Interestingly, in Hole 528 phillipsite occurs even in rhyolitic? pumice layers which are compositionally very close to the volcanoclastic rocks of Hole 525A, even though one could expect clinoptilolite as alteration product of the glass. Clinoptilolite, a high-silica zeolite, generally grows rather slowly (Kastner, 1981), in contrast to phillipsite, whose abundant inclusions of, for example, cryptocrystalline clay minerals or matrix indicate rapid growth. The absence of clinoptilolite, even in highly differentiated pumice layers of Hole 528, is probably due

to percolating pore solutions from the over- and underlying tholeiitic basalts, but could also be due to the slow growth rates which "handicap" clinoptilolite in the presence of phillipsite. Changes in the composition of zeolites throughout the alteration process are rather likely, but that are not recognizable by thin-section microscopy, although changes in crystal shapes are visible. However, the different crystal shapes of phillipsite (small and fibrous versus large and platy) could equally well reflect different growth rates.

The geochemical importance of the rocks studied is in some respect dependent on the correctness of the foregoing discussion. If we are right in believing that the bulk of the tephra in the volcanoclastic sediments was derived from high-standing seamounts (shallow-water), partly emergent as ocean islands, a comparison with basalts formed during the same time at nearby ridge crests will contribute to our understanding of source differences between magmas from ocean islands and those in ridge settings. Interpretation of the chemical composition of volcanoclastic sediments is strongly constrained by the potentially severe redistribution of the elements in the dominantly glassy clasts with their high surface/volume ratios and by the additional possibility of pre-depositional weathering. Further complexities arise because of the mixing of compositionally diverse volcanic and nonvolcanic clasts before and during transport.

We have argued that despite these limitations the composition of the volcanoclastic rocks is similar in two main respects to that of the basement basalts from the same sites studied by Richardson et al. (this volume). First, the composition of the rocks is much more evolved than that of most MORB, as is shown by low abundances of compatible elements. The rock composition is distinctly more differentiated than the composition of similar volcanoclastic rocks drilled south of the Canary Islands during Leg 47A (Schmincke and von Rad, 1979); we have chemically analyzed these Leg 47A rocks in detail (unpubl.). Indeed, basalts dredged along the Walvis Ridge appear to be in general distinctly more evolved than MORBs, as is shown by the data of Humphris and Thompson (1982). Thus, magmas in the storage reservoirs beneath the Walvis Ridge mantle magma system were efficiently fractionated before eruption. This is not uncommon in oceanic islands but is more unusual for the ridge settings. Interestingly, the basement lavas show different degrees of evolution: the crest site basalts at Hole 525A are significantly more evolved than most of those at the flank Site 528. These differences are mirrored by the more evolved compositions (determined mostly by textural and mineralogical evidence) of Hole 525A compared to Hole 528 volcanoclastic rocks. This conclusion supports but does not prove that magma chamber evolution for the Walvis Ridge and seamount/island settings was similar.

A second feature of Walvis Ridge basalts is their large abundance in "incompatible" major and trace elements, much higher than explainable by fractionation (see Richardson et al., this volume; Humphris and Thompson, 1982). Although more constrained (for example, by large uptake of K and Rb during alteration),

our data are compatible with the interpretation that Walvis Ridge magmas were derived from enriched mantle sources. Moreover, source compositions have changed in space and time. For example, Zr/Nb ratios decreased from about 10 at the presumed older, eastern end to about 6 in the central section; Tristan da Cunha basalts further to the west have ratios around 4 (Humphris and Thompson, 1982). Sites drilled during Leg 74 are in the western part of the eastern segment but show pronounced decreases from the Ridge Site 525 toward the northwestern flank sites (Zr/Nb  $\approx$  10 to 5-7, Richardson et al., this volume; 5-6, our data), covering the range reported by Humphris and Thompson (1982). Thus, whether or not there is a spatial and temporal decrease from east to west, as suggested by Humphris and Thompson (1982), our Site 528 Zr/Nb ratios closely correspond to those in the underlying basalts analyzed by Richardson et al. (this volume), supporting the view that the ridge and seamount/ocean island magmas were derived from the same type of mantle source. The volcanoclastic rocks of Hole 525A have now been sampled in more detail, in order to study their chemistry in comparison with that of basalts from this site.

In summary, our preliminary and incomplete study of some of the volcanoclastic sediments drilled during Leg 74 along a transect across the northern flank of the central Walvis Ridge indicates

a) There was a process of growth and decay of seamounts, at some stage emergent islands, during a period of about 2 m.y.

b) Tephra recovered in deep sea sediments is dominantly glassy and highly vesicular, derived from shallow marine eruptions modified and transported as turbidity currents to greater depths.

c) Highly differentiated trachytic? magmas evolved near Site 525.

d) Basement accretion and seamount/island growth are clearly related in time, space, and composition. Evidence for this is found in (1) interlayered volcanoclastic sediments and basalt flows, (2) similarity in degree of magma evolution, and (3) similarity in mantle source compositions.

e) Postdepositional, low-temperature alteration of the glass-rich volcanoclastic sediments was severe, with transformation of the mafic glasses into smectite and phillipsite controlled by diffusion as well as by solution-precipitation processes. These last processes dominate in the silicic/alkalic glasses, where clinoptilolite (rare phillipsite) precipitated, and in plagioclase, which is altered into phillipsite and adularia, the last reflecting K-rich percolating pore solutions. Except for major uptake of K and Rb and loss of Ca and Fe, the systems remained sufficiently closed to redistribution of the elements to retain recognizable chemical characteristics.

#### ACKNOWLEDGMENTS

We thank H. Fütterer, Kiel, for providing the samples and photographs of core material and S. Richardson for a preliminary copy of his chapter on the composition of basement lavas. R. Neuser, Bochum, did the cathodoluminescence studies. XRF-analyses were carried out by H. Niephaus, Bochum. H. Fichtbauer, Bochum, and U. von Rad, Hannover, kindly reviewed the manuscript. The work was sup-

ported by the Deutsche Forschungsgemeinschaft, Grants Schm 250/26, 28-8, priority research "Deep Sea Drilling."

REFERENCES

- Alietti, A., 1972. Polymorphism and crystal chemistry of heulandites and clinoptilolites. *Am. Mineral.*, 57:1448-1462.
- Baker, P. E., Gass, I. G., Harris, P. G., and LeMaitre, R. W., 1964. The volcanological report of the Royal Society expedition to Tristan da Cunha, 1962. *Phil. Trans. R. Soc. London, Ser. A.*, 256:439-578.
- Boles, J. R., 1972. Composition, optical properties, cell dimension, and the thermal stability of some heulandite group zeolites. *Am. Mineral.*, 57:1463-1493.
- Humphris, S. E., and Thompson, G., 1982. A geochemical study from rocks of the Walvis Ridge, South Atlantic. *Chem. Geol.*, 36:253-274.
- Kastner, M., 1971. Authigenic feldspars in carbonate rocks. *Am. Mineral.*, 56:1403-1442.
- , 1981. Authigenic silicates in deep-sea sediments: Formation and diagenesis. In Emiliani, C. (Ed.) *The Sea* (Vol. 7). *The Oceanic Lithosphere*: London (Academic Press), 915-980.
- Kastner, M., and Siever, R., 1979. Low-Temperature feldspars in sedimentary rocks. *Am. J. Sci.*; 279:435-479.
- Kelts, K., and McKenzie, J. A., 1976. Cretaceous volcanogenic sediments from the Line Islands Chain: Diagenesis and formation of K-feldspar, DSDP Leg 33, Hole 315A and Site 316. In Schlanger, S. O., Jackson, E. D., et al., *Init. Repts. DSDP*, 33: Washington (U.S. Govt. Printing Office), 789-831.
- LeMaitre, R. W., 1962. Petrology of volcanic rocks, Gough Islands, South Atlantic. *Geol. Soc. Am. Bull.*, 73:1309-1340.
- Moore, J. G., and Schilling, J. G., 1973. Vesicles, water and sulfur in Reykjanes Ridge basalts. *Contr. Mineral. Petrol.*, 41:105-118.
- Mumpton, F. A., 1960. Clinoptilolite redefined. *Am. Mineral.*, 45:351.
- Reynolds, C. R., and Hower, J., 1970. The nature of interlayering in mixed-layer illite-montmorillonite. *Clays Clay Min.*, 18:25-36.
- Riech, V., 1979. Diagenesis of silica, zeolites, and phyllosilicates at Sites 397 and 398. In von Rad, U., Ryan, W. B. F., et al., *Init. Repts. DSDP*, 47, Pt. 1: Washington (U.S. Govt. Printing Office), 741-759.
- Schmincke, H.-U., and von Rad, U., 1979. Neogene evolution of Canary Island volcanism inferred from ash layers and volcanoclastic sandstones of DSDP Site 397 (Leg 47A). In von Rad, U., Ryan, W. B. F., et al., *Init. Repts. DSDP*, 47, Pt. 1: Washington (U.S. Govt. Printing Office), 703-725.
- Zinkernagel, U., 1978. Cathodoluminescence of quartz and its application to sandstone petrology. *Contr. Sedimentol.*, 8:1-69.

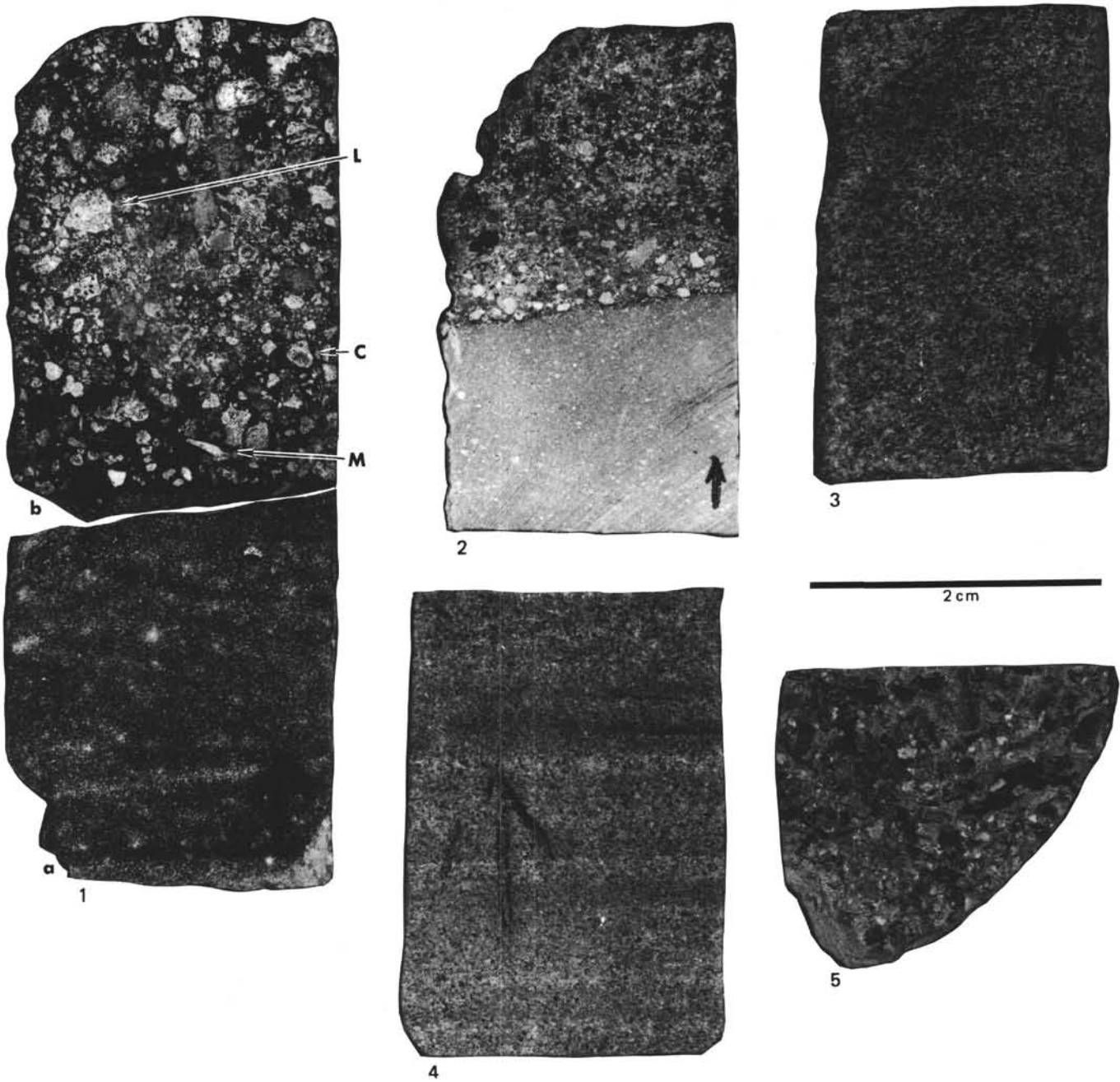
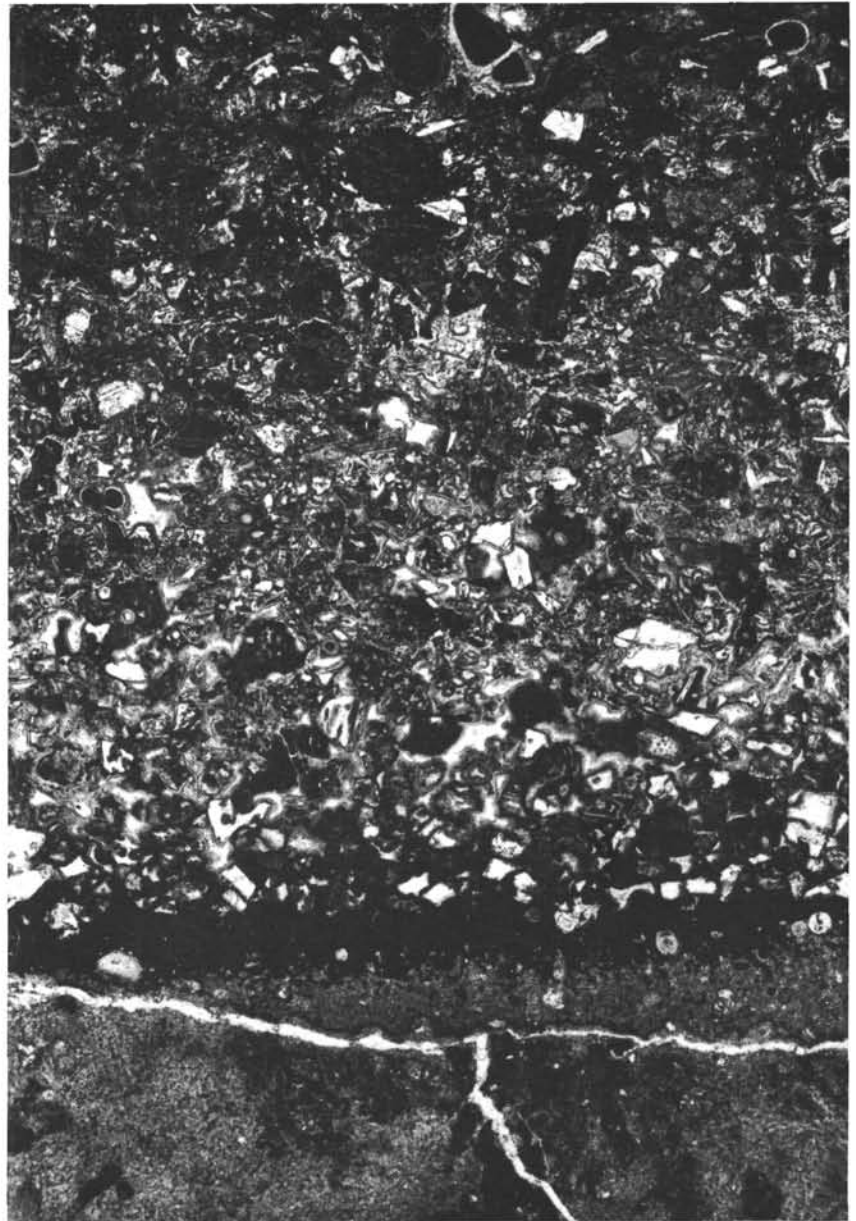


Plate 1. Photographs of thin-section chips (arrow shows up). 1. Sample 528-37-2, 38-40 cm. Cross-bedded spalling-shard tuff, overlain by poorly sorted lithic (L) and crystal-rich layer, with a matrix consisting of spalling shards and clay. Note dark, hollow interior of feldspar clasts (C) and large molluscan shell fragment (M) at the base of layer b. 2. Sample 528-37-1, 135-138 cm. Contact of a nannofossil chalk (below) and a volcaniclastic layer enriched at the base in rounded lithic clasts; light-colored clasts are trachyte?, dark-colored are tachylite and smectitized glass. 3. Sample 528-37-7, 14-17 cm. Fine, sandy, volcaniclastic rock, showing dark vitric and tachylitic clasts surrounded by zeolitic matrix. 4. Sample 528-37-6, 129-132 cm. Fine-grained volcaniclastic rock showing distinct bedding and strongly zeolitized areas (white-gray) parallel to bedding. 5. Sample 525A-46-4, 46-53 cm. Base of a coarse-grained layer showing greenish (dark) fragments of former glass shards, now totally altered to clay minerals, and white K-feldspar clasts (sanidine).



2 cm



2 mm

Plate 2. Sample 528-37-7, 42-46 cm. 1. Contact of a basal nannofossil chalk and overlying volcaniclastic rock. The bedding structures of the volcaniclastic sediment are accentuated by strongly smectitized dark areas at the base of the volcaniclastic layer. 2. Microphotograph of same sample, showing the contact and the strongly smectitized basal layer of the volcaniclastic rock, with fibrous smectite surrounding spalling shards which are now totally dissolved. The black layer at the contact is rich in Mn/Fe oxides/hydroxides.

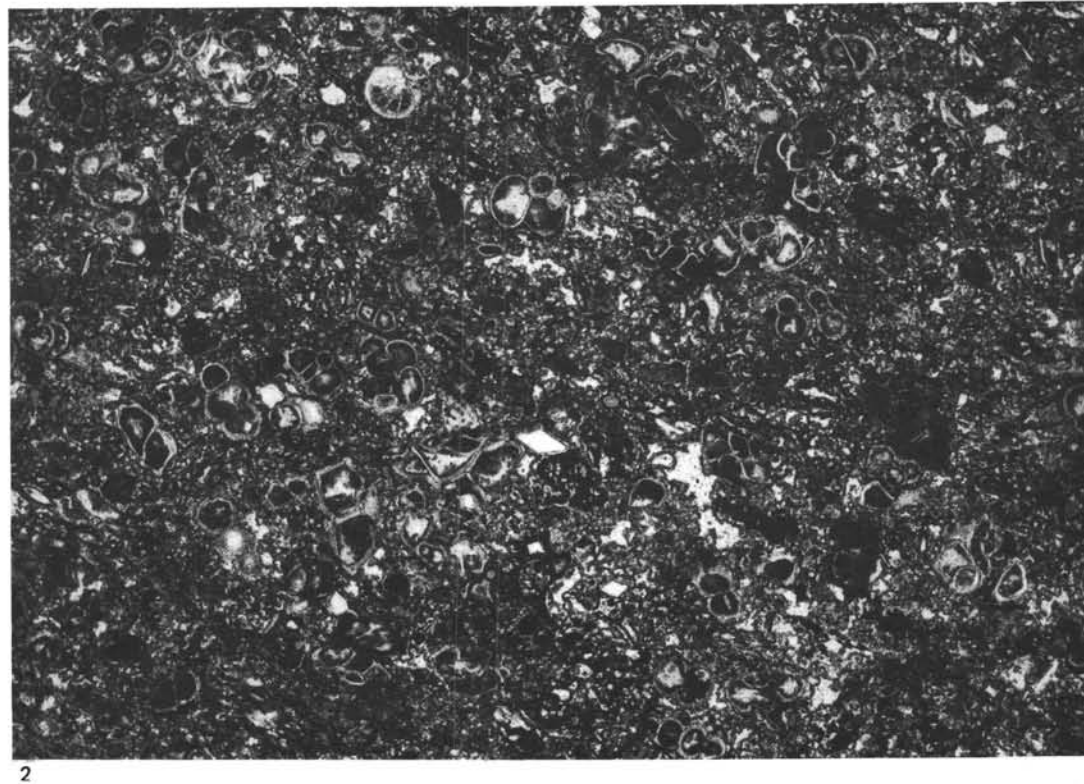
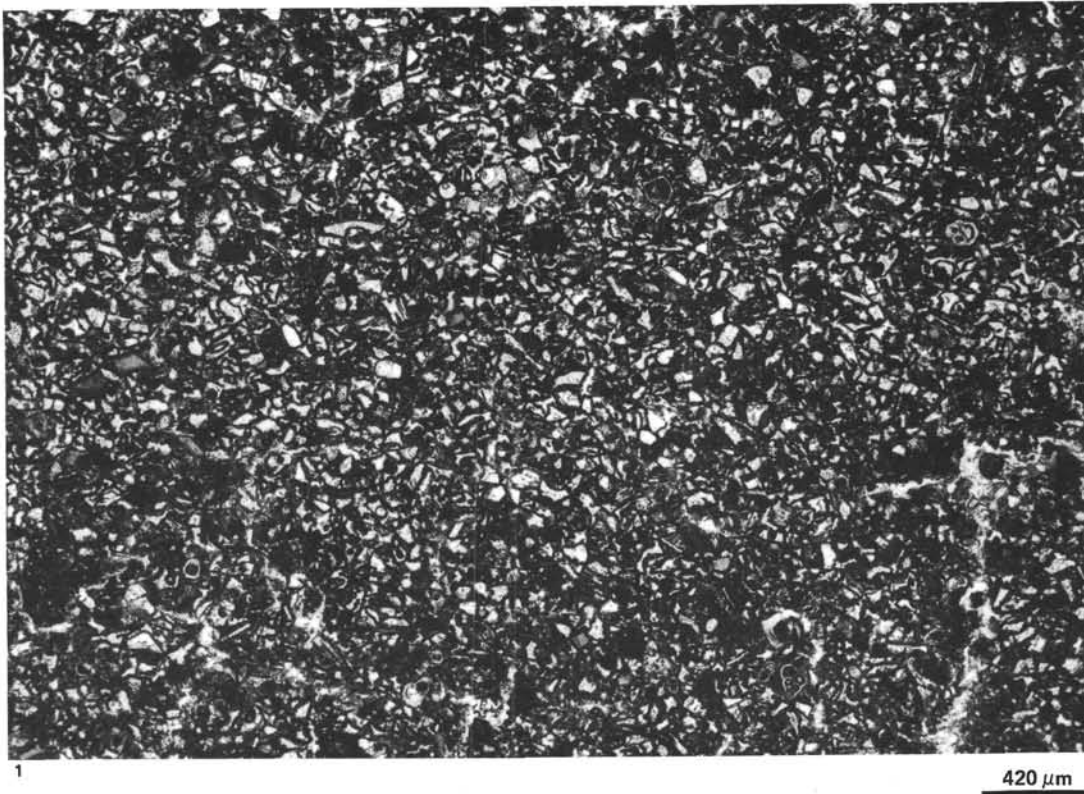


Plate 3. Overview-microphotographs of fine-grained volcaniclastic rocks. 1. Sample 528-37-2, 34–37 cm. Spalling-shard tuff, showing well-sorted spalling shards, marginally rimmed by dark smectite. Most shards are completely dissolved, but strongly hydrated and “palagonitized” shards are also present (center left). Elongated shards are arranged slightly parallel to the bedding (i.e., parallel to the length of the photo). Primary pore space is mostly filled with smectite. A few foraminifers are dispersed throughout the layer. 2. Sample 528-37-4, 111–114 cm. Volcaniclastic rock extremely rich in foraminifers. The fine-grained volcanic particles are small spalling shards (strongly smectitized). Chambers of foraminifers are mostly filled with glauconite? and Mn/Fe oxides/hydroxides.

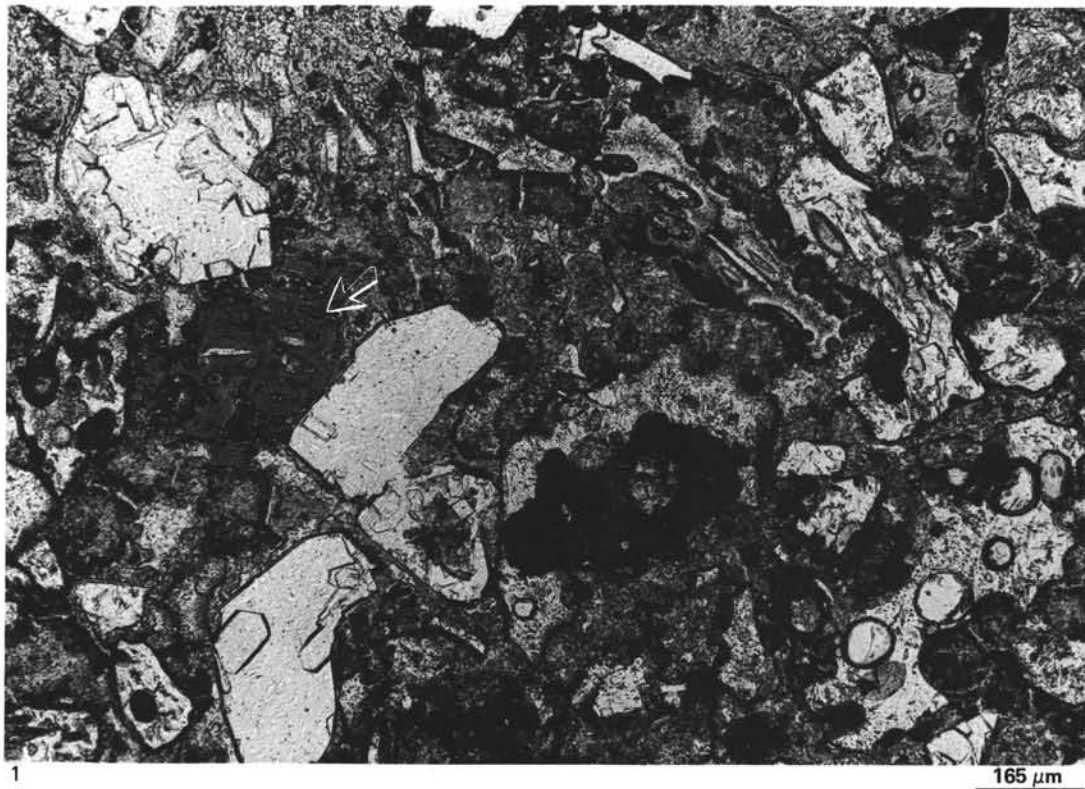


Plate 4. 1. Sample 528-37-3, 8–11 cm. Photomicrograph of scoria shards, vesicular tachylite, and dissolved feldspar clasts in a matrix of small spalling shards and smectitized ash. Hollows of former feldspar clasts are partly filled with phillipsite cement. Scoria shards are zeolitized following marginal smectitization. Note oxidized “fresh” glass shard (arrow) with acicular plagioclase microphenocrysts. 2. Sample 528-37-3, 18–20 cm. Photomicrograph of scoria shard and tachylite tuff. Note elongated vesicles in large zeolitized scoria shard (center left) and plagioclase phenocryst in tachylite (center right).

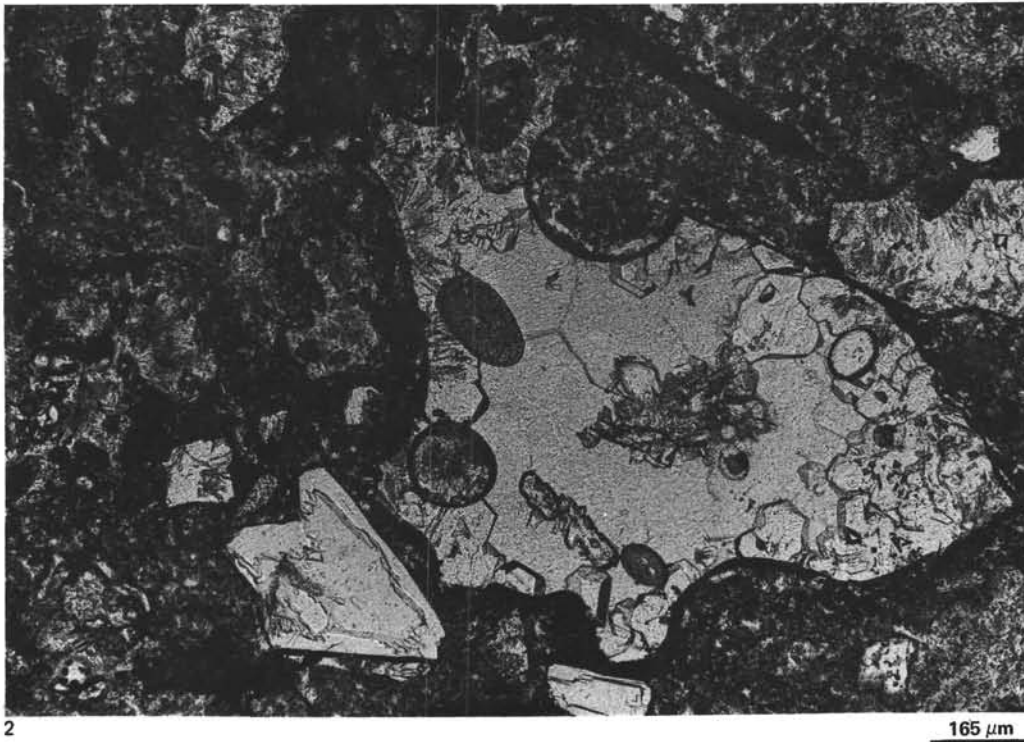
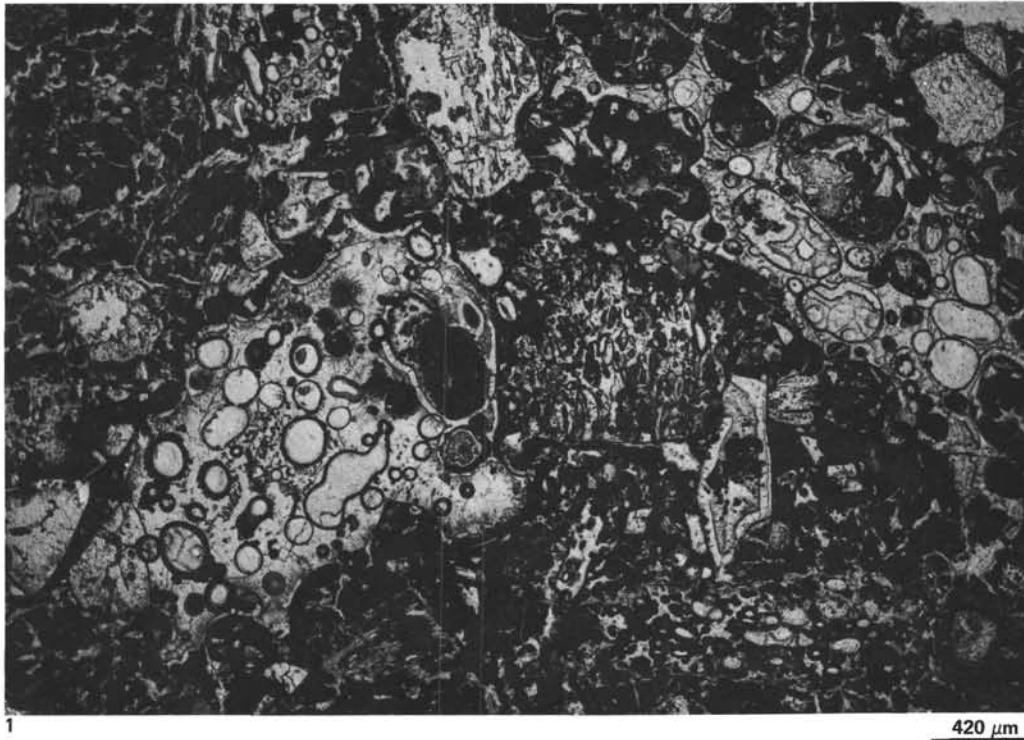


Plate 5. 1. Sample 528-37-2, 37–40 cm. Photomicrograph of very large, highly vesicular scoria? shards and smaller feldspar clasts in a groundmass of small spalling shards and smectite. The irregularly shaped shard in the upper right shows sharp pointed edges and different sizes of vesicles, perhaps representing two generations of vesiculation. The large shard in the left shows coalescing bubbles which are calcite-cemented. All shards show a sequence of zeolites: (a) light-colored thomsonite (?) forming a palisadelike rim inside the shards and vesicles, followed by (b) light gray fibrous phillipsite which passes into thick, stout phillipsite. 2. Sample 528-43-1, 23–26 cm. Photomicrograph of large scoria shard with zircon crystal in a matrix of smectitized fine ash. Because of thorough alteration, only vesicles in marginal areas are preserved. Alteration has taken place in at least 4 steps: (a) rim of smectite and Mn/Fe oxides/hydroxides; (b) growth of fibrous, bunched phillipsite followed by prismatic phillipsite; (c) dissolution of the remaining glass; and (d) cementation of the new pore space by calcite enclosing “dust” which remained from dissolution in the center of the shard.

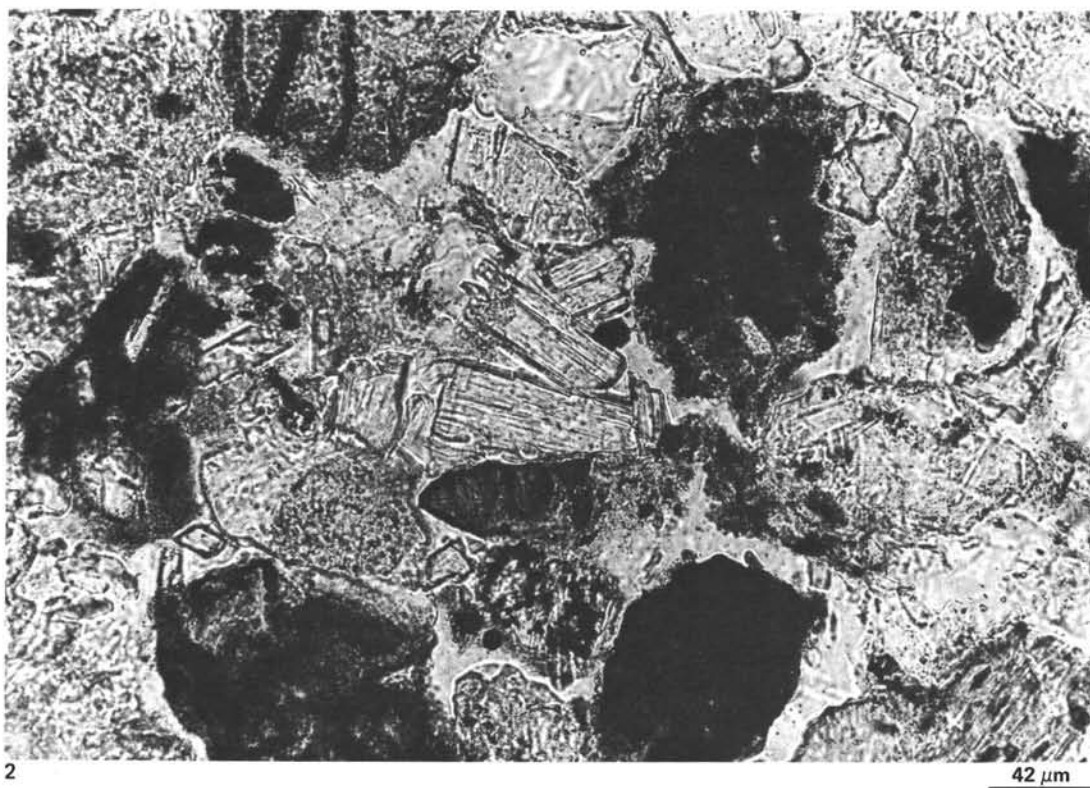
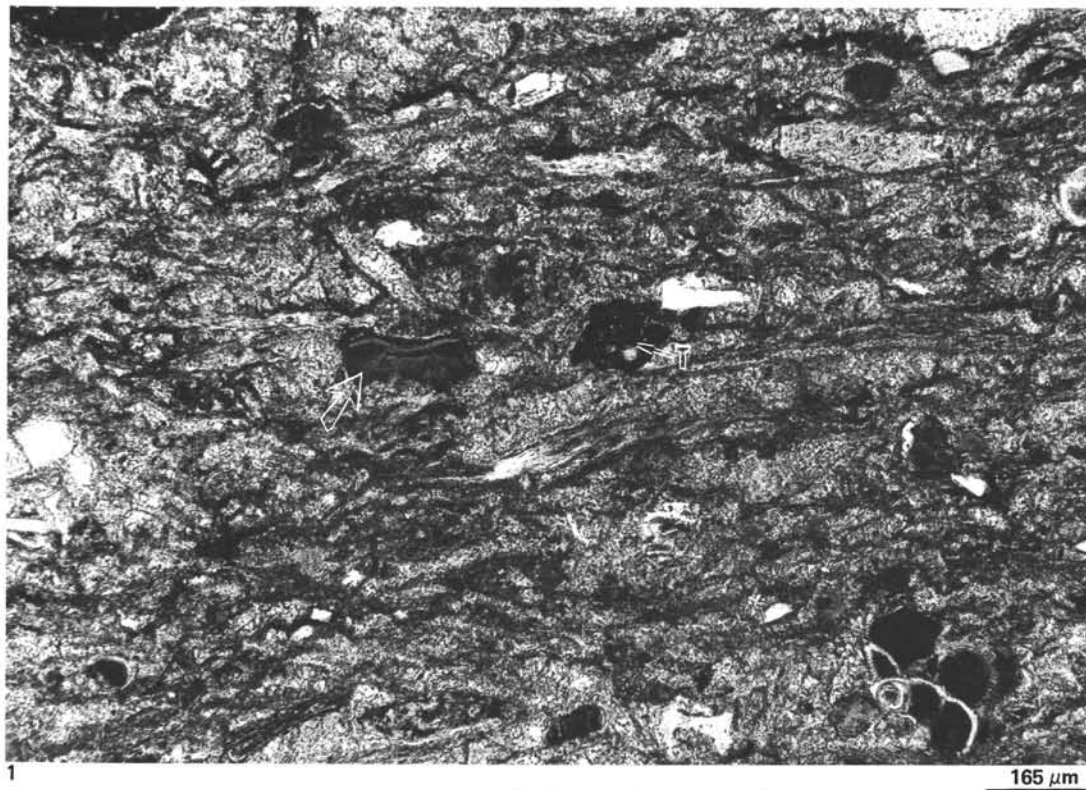


Plate 6. 1. Sample 528-41-1, 57-61 cm. Photomicrograph of pumice tuff, slightly elongated pumice shards being oriented parallel to bedding. After marginal replacement of glass by light-colored smectite, the remaining glass was partly dissolved and the new pore space filled by small phillipsite crystals. Note single, dark, "palagonitized" sideromelane shard (arrow) and tachylite (T) in the center of the photograph. Foraminifers have glauconite?-filled chambers (lower right). 2. Sample 525A-51-2, 95-104 cm. Photomicrograph of trachytic? volcanoclastic rock, showing platy clinoptilolite in primary pore space.

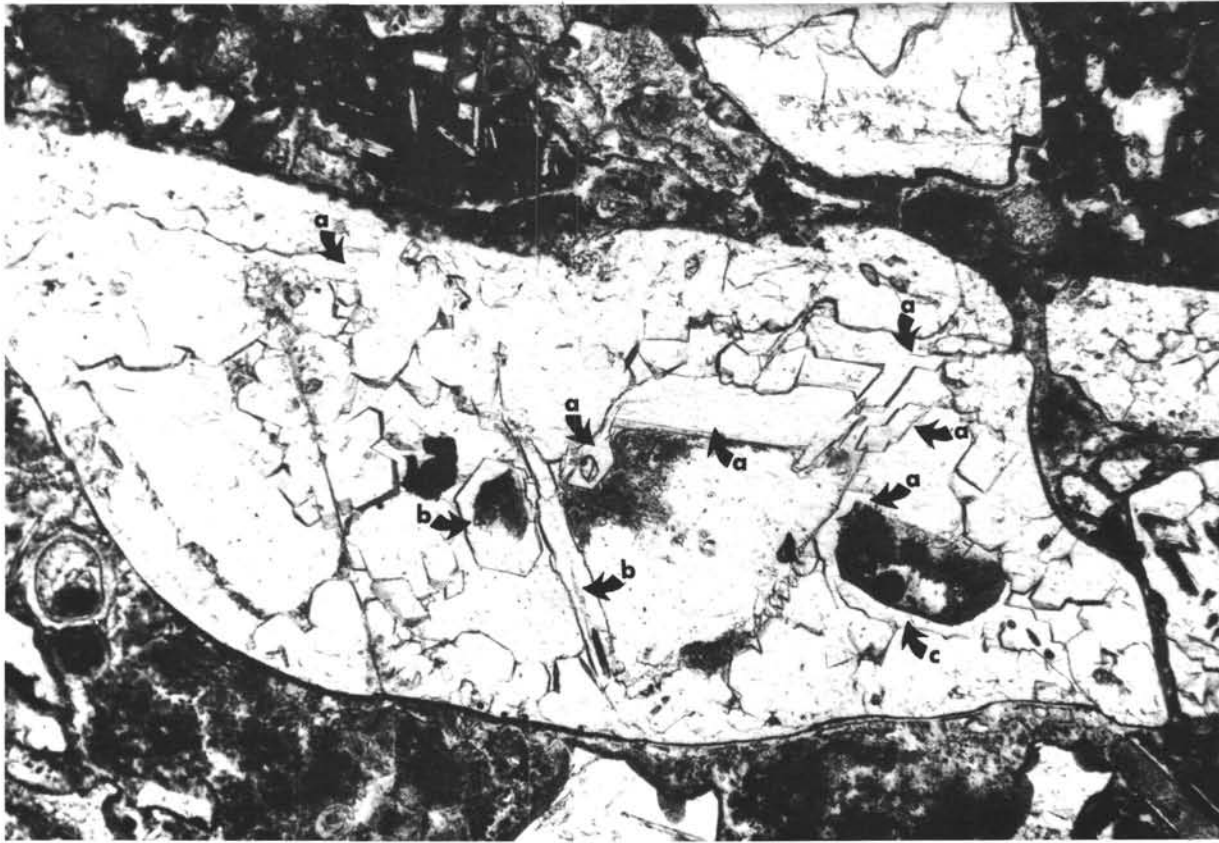
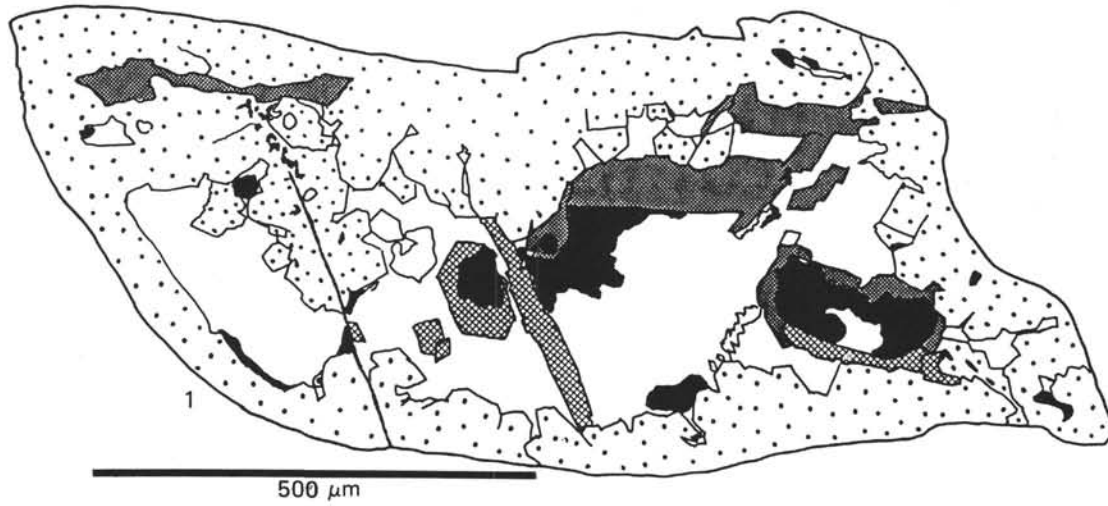


Plate 7. 1-2. Sample 528-37-3, 18-20 cm. Photomicrograph (2) and drawing (1) of alteration features of rounded feldspar clast. The drawing shows different alteration phases (stippled area = phillipsite; black area = smectite; wide and narrow checkered fields show areas of K-feldspar extinguishing simultaneously). Areas marked a, b, and c, are feldspar domains extinguishing simultaneously.

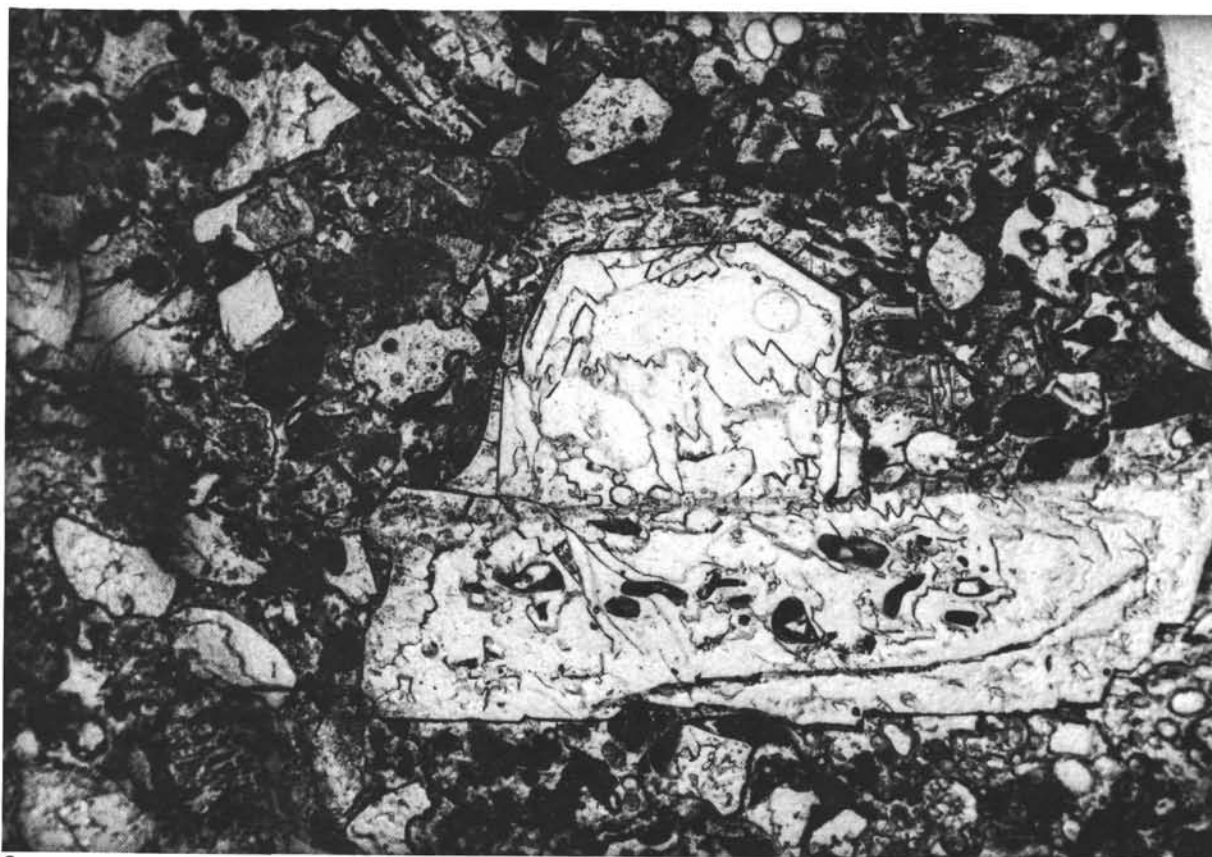
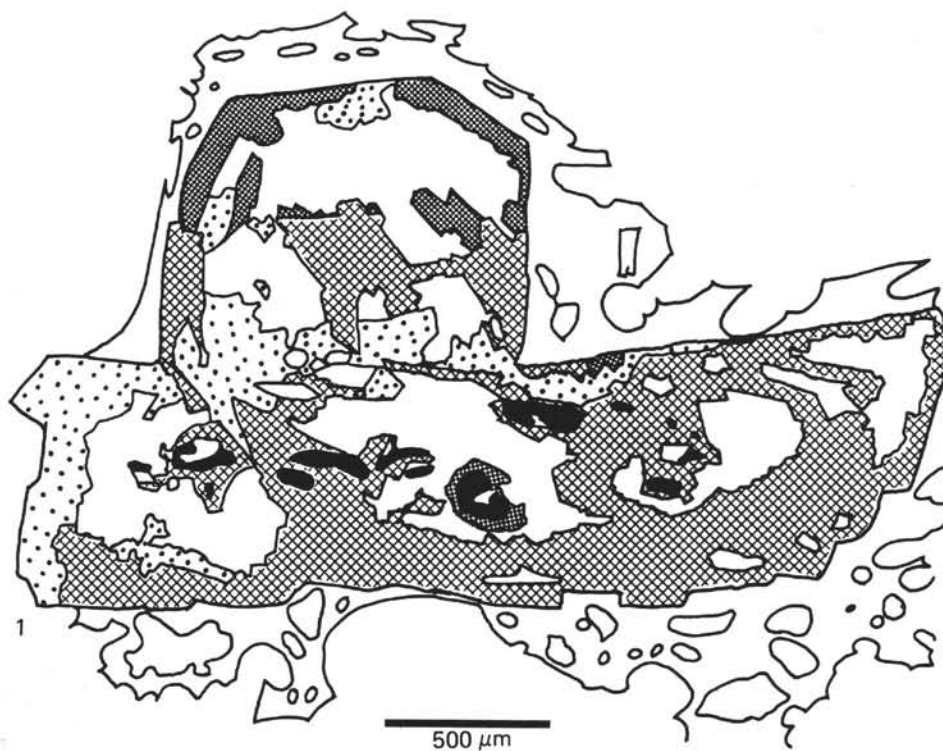


Plate 8. 1-2. Sample 528-37-3, 18-20 cm. Photomicrograph (2) and drawing (1) of alteration features of feldspar. The euhedral phenocryst is surrounded by a formerly glassy, now altered, rim. On the drawing, the clear area (outside phenocryst) represents the former glass rim; stippled area = phillipsite; wide and narrow checkered areas are authigenic? K-feldspar extinguishing simultaneously; dark area = former glass inclusions; clear areas inside feldspar are hollow.



1

250  $\mu\text{m}$ 

2

Plate 9. 1. Sample 528-37-1, 135-138 cm. Photomicrograph showing tachylite with dissolved olivine phenocrysts (lower left) and clast of hydrated sideromelane with phenocryst aggregates of olivine and plagioclase (now dissolved) and plagioclase microlaths. 2. Sample 528-37-2, 37-40. Photomicrograph of rounded feldspar, partly surrounded by a glassy rim. Both glass and feldspar are altered; feldspar is replaced by albite? and phillipsite, and some parts are hollow. Glass is marginally smectitized followed by phillipsite replacing the remaining glass.